Unveiling the transferability of PLSR models for leaf trait estimation: lessons from a comprehensive analysis with a novel global dataset

Fujiang Ji [1*], Fa Li [1*], Dalei Hao [2], Alexey N. Shiklomanov [3], Xi Yang [4], Philip A. Townsend [1], Hamid Dashti[1], Tatsuro Nakaji [5], Kyle R. Kovach[1], Haoran Liu [1], Meng Luo [1], Min Chen[1]

[1] Department of Forest and Wildlife Ecology, University of Wisconsin-Madison, 1630 Linden Drive, Madison, WI, USA; [2] Atmospheric Sciences and Global Change Division, Pacific Northwest National Laboratory, Richland, WA, USA; [3] NASA Goddard Space Flight Center, 8800 Greenbelt Rd., Building 33, Greenbelt, MD, 20771, USA; [4] Department of Environmental Sciences, University of Virginia, Charlottesville, VA, USA; [5] Uryu Experimental Forest, Hokkaido University, Moshiri, Horokanai, Hokkaido 074-0741, Japan

Author for correspondence:

Fujiang Ji *(Email: fujiang.ji@wisc.edu)* ***and Min Chen*** *(Email: min.chen@wisc.edu)*

[*] These authors contributed equally.

Summary

- Leaf traits are essential for understanding many physiological and ecological processes. Partial least-squares regression (PLSR) models with leaf spectroscopy are widely applied for trait estimation, but their transferability across space, time and plant functional types (PFTs) remains unclear.
- We compiled a novel dataset of paired leaf traits and spectra, with 47,393 records for >700 species and eight PFTs at 101 globally-distributed locations across multiple seasons. Using this dataset, we conducted an unprecedented comprehensive analysis to assess the transferability of PLSR models in estimating leaf traits.
- While PLSR models demonstrate commendable performance in predicting chlorophyll content, carotenoid, leaf water and leaf mass per area prediction within their training data space, their efficacy diminishes when extrapolating to new contexts. Specifically, extrapolating to locations, seasons, and PFTs beyond the training data leads to reduced R^2 (0.12-0.49, 0.15-0.42, and 0.25-0.56) and increased *NRMSE* (3.58-18.24%, 6.27-11.55% and 7.0-33.12%) compared to nonspatial random cross-validation (NRCV). The results underscore the importance of incorporating greater spectral diversity in model training to boost its transferability.
- These findings highlight potential errors in estimating leaf traits across large spatial domains, diverse PFTs and time due to biased validation schemes and provide guidance for future field sampling strategies and remote sensing applications.

Keywords

Leaf traits, Leaf spectroscopy, Partial least-squares regression (PLSR), Transferability, Cross-validation.

Introduction

Leaf traits play an important role in modulating plant physiological processes and ecosystem biophysical and biochemical dynamics (Wright *et al.*, 2004; Violle *et al.*, 2007, 2014; Ustin *et al.*, 2009; Kattge *et al.*, 2011; Yi *et al.*, 2014). For example, chlorophyll content influences leaf-absorbed solar energy and is therefore closely related to plant photosynthesis (Croft *et al.*, 2013). Carotenoid pigments are associated with the xanthophyll cycle, a key mechanism for preventing plant photooxidative stress under drought, heat stress, and high light conditions (Ruban *et al.*, 2007). Leaf water content is a useful indicator of overall plant water status and therefore health and productivity (Wright *et al.*, 2004; Cheng *et al.*, 2011; Pereira *et al.*, 2013; Cavender-Bares *et al.*, 2020). Leaf mass per area (LMA) is indicative of a wide variety of plant trade-offs related to investment in leaf construction vs. photosynthesis (Poorter *et al.*, 2009) and determines plant ecological strategy (Osnas *et al.*, 2013; Puglielli *et al.*, 2015). Therefore, quantifying and understanding the spatiotemporal variations of leaf traits is essential for improving our prediction of the effects of environmental changes on terrestrial ecosystems.

Leaf traits are known to vary due to environmental heterogeneity (Messier *et al.*, 2010, 2017; Albert *et al.*, 2010; Jung, 2022) This variations is driven by both biotic factors such as plant functional types (PFTs), species, phenology, leaf age and leaf development stage, as well as abiotic determinants like the availability and variability of resources including nutrients, water, and energy, etc.) (Stein & Kreft, 2015; Chavana-Bryant *et al.*, 2017; Wu *et al.*, 2017; Serbin *et al.*, 2019c; Regos *et al.*, 2022). Direct measurements of leaf traits using laboratory techniques are typically challenging and labor-intensive. Fortunately, many studies have demonstrated the capability of leaf spectroscopy to accurately and efficiently estimate leaf traits (Chavana-Bryant *et al.*, 2013; Dahlin *et al.*, 2013; Asner *et al.*, 2015; Wang *et al.*, 2015; Yang *et al.*, 2016; Meerdink *et al.*, 2016; Sun *et al.*, 2018; Hill *et al.*, 2019; Féret *et al.*, 2019, 2021; Nakaji *et al.*, 2019; Serbin *et al.*, 2019c; Fu *et al.*,

2020; Streher *et al.*, 2020; Spafford *et al.*, 2021; Jiang *et al.*, 2021; Yan *et al.*, 2021; Chen *et al.*, 2022; Wan *et al.*, 2022). Leaf traits are often estimated from spectra by fitting physics-based models or data-driven models (Clevers & Gitelson, 2013; Féret *et al.*, 2019; Spafford *et al.*, 2021; Wang *et al.*, 2021; Angel & Shiklomanov, 2022). Physics-based models, also known as radiative transfer models (RTMs), rely on the predefined physical mechanisms of the interaction between electromagnetic radiation and leaf constituents (Jacquemoud & Baret, 1990; Jacquemoud *et al.*, 1996; Feret *et al.*, 2008; Féret *et al.*, 2017, 2019; Wu *et al.*, 2021). In theory, RTMs are site- and species-independent, resulting in high robustness and transferability (Jacquemoud & Baret, 1990; Feret *et al.*, 2008; Kimes *et al.*, 2009; Berger *et al.*, 2018; Spafford *et al.*, 2021). However, in practice, many RTM coefficients (e.g., specific absorptivities, refractive index) are actually empirically calibrated (Wang *et al.*, 2015, 2021; Verrelst *et al.*, 2019), and moreover, the RTM inversion problem is often "ill-posed" because different combinations of traits can produce similar leaf reflectance (Combal *et al.*, 2003; Lewis & Disney, 2007; Wang *et al.*, 2015, 2021; Féret *et al.*, 2017; Berger *et al.*, 2018; Verrelst *et al.*, 2019).

Data-driven approaches developed for leaf traits estimation include simple regression with spectral vegetation indices (Fassnacht *et al.*, 2015; Moharana & Dutta, 2016; Jay *et al.*, 2017), more advanced statistical methods like wavelet transforms (Blackburn, 2007; Cheng *et al.*, 2011; Banskota *et al.*, 2015), Partial-Least Squares Regression (PLSR) (Wold *et al.*, 1984; Asner & Martin, 2008; Serbin *et al.*, 2012; Verrelst *et al.*, 2019) and machine learning methods (Hornik *et al.*, 1989; Breiman, 2001; Rasmussen, 2004; Smola & Schölkopf, 2004; Verrelst *et al.*, 2012). In particular, PLSR is widely favored for its high accuracy, ease of implementation and interpretation, ability to deal with high dimensional data, and long history of use in chemometrics (Thenkabail *et al.*, 2013; Fu *et al.*, 2020). The most popular method for retrieving plant traits from spectra is PLSR, which has been used extensively over the past two decades (Townsend *et al.*, 2003; Martin *et al.*, 2008;

Yang *et al.*, 2016; Nakaji *et al.*, 2019; Serbin *et al.*, 2019c; Fu *et al.*, 2020; Yan *et al.*, 2021; Wan *et al.*, 2022). However, these empirical data-driven methods could have important limitations, the test practices for data-driven statistical analysis dictate that predictive models should only be applied – would only be expected to provide accurate results for – new measurements that fall within the range of the data used to train the predictive models. Moreover, current literature is inconclusive on the generalizability or transferability of PLSR for leaf trait estimation. Some studies show that PLSR studies with relatively confined spatial extents show good accuracy (Yang *et al.*, 2016; Meerdink *et al.*, 2016; Wu *et al.*, 2017; Chen *et al.*, 2022; Kothari *et al.*, 2022b), but PLSR studies over larger and more diverse areas are rare. One such study (Serbin *et al.*, 2019c) shows that a single PLSR model achieves good accuracy for LMA estimates across a wide phylogenetic, geographic, and climatic range (woody and herbaceous species in the Americas over a range spanning Arctic Alaska to the Colombian Amazon). On the other hand, a study of four species typical of coastal sand dune grasslands along the Belgian North Sea coast (Helsen *et al.*, 2021) found significantly lower accuracy for across-species PLSR models than species-specific PLSR models for retrieving LMA. Another study (Heckmann *et al.*, 2017) investigated the transferability of models between the Brassicaceae genera *Moricandia* and *Brassica*. The findings revealed significantly low transferability, indicating that model transferability does not strictly correlate with phylogenetic proximity. Additional evidence for the lack of generality of PLSR models is the variability in coefficients and choice of most important wavelengths across studies (Knyazikhin *et al.*, 1998; Wessels *et al.*, 2012; Croft *et al.*, 2013; Yang *et al.*, 2016; Chlus & Townsend, 2022b).

As both field spectroscopy and remote (UAV, airborne, satellite) imaging spectroscopy become more common — especially in the context of current and upcoming global satellite imaging spectroscopy missions like Hyperspectral Imager SUite (HiSUI, (Iwasaki *et al.*, 2011)) and the PRecursore IperSpettrale della Missione Applicativa

(PRISMA, (Loizzo *et al.*, 2019)), Environmental Monitoring and Analysis Program (EnMap, (Guanter *et al.*, 2015)), Copernicus Hyperspectral Imaging Mission for the Environment (CHIME, (Nieke & Rast, 2018)), and NASA's Surface Biology and Geology (SBG, (Cawse-Nicholson *et al.*, 2021)) — understanding the generalizability of data-driven methods for estimating traits from spectra is essential and timely. This is especially the case given the unprecedented volume of field spectroscopy data available today, covering a wide spatial and phylogenetic range. As well, model evaluations in most published works are primarily based on nonspatial random cross-validation (NRCV) with limited sites. The NRCV may induce a better estimation of model performance, potentially because of its failure to account for spatial, temporal, and PFTs autocorrelation in the data (Meyer *et al.*, 2019; Ploton *et al.*, 2020).

Here, we present two main questions: (1) How well do the PLSR models transfer to new domains (new sites, PFTs and time)? (2) What are the potential factors influencing the transferability of PLSR? We investigated the transferability and performance of PLSR using various validation strategies, with the aim of providing insights into its suitability for different application scenarios. First, we synthesized a novel global dataset of both direct measurements of leaf traits (i.e., chlorophyll, carotenoids, leaf mass per area and equivalent water thickness) and the corresponding leaf reflectance measurements with 47,393 records for more than 700 species and eight PFTs at 101 globally-distributed locations across multiple seasons. Then, we evaluated the transferability of PLSR through space, through time, and across PFTs, comparing random, spatiotemporal, and across-PFT cross-validation methods. Finally, we investigated the impacts of potential factors (climate zones and spectral diversity) that affect the transferability of PLSR. We posed the hypotheses for the analysis: (1) predictive models can expect accurate trait predictions for new measurements falling within the range of the data used during model training and the model

performance will decline when extrapolating to new domains; (2) greater spectral diversity in model training means better predictability of the PLSR models in new domains.

Materials and Methods

2.1 The compiled dataset

We synthesized 37 datasets from published literatures and the EcoSIS Spectral Library (https://ecosis.org/) (Hosgood *et al*., 1994; Jacquemound *et al*., 2003; Singh, 2013; Serbin & Townsend, 2014; Serbin *et al*., 2014, 2017, 2018, 2019a,b,c,d, 2021; Couture, 2015, 2016; Couture *et al*., 2015; Meerdink, 2016; Serbin, 2016; Serbin & Rogers, 2016; Yang *et al*., 2016; Kattenborn *et al*., 2017; Wu *et al*., 2017; Ely *et al*., 2018, 2019; Kamoske *et al*., 2018; Chlus, 2019; Wang, 2019a,b, 2022; Wu; *et al*., 2019a,b; Ge *et al*., 2019; Wu *et al*., 2019; Nakaji *et al*., 2019; Grzybowski *et al*., 2020; Helsen *et al*., 2020a,b; Burnett *et al*., 2021b,c,d,e; Villa *et al*., 2021a,b; Chlus & Townsend, 2022a,b; Kothari *et al*., 2022a,b,c; Chen *et al*., 2022), compiling a new dataset that covers all major biomes and climate zones over the world (Fig. 1a; Fig. S1, Table S1). The compiled dataset contained both common leaf traits and the corresponding leaf reflectance measurements with 47,393 records for more than 700 species and eight PFTs at 101 globally-distributed locations (Fig. 1b, Fig. S2), and some of the records covered seasonal measurements of leaf traits and spectra. First, we categorized the species in the dataset into 8 different PFTs: evergreen needleleaf forests (ENF, n = 891), evergreen broadleaf forests (EBF, n = 1,382), deciduous needleleaf forests (DNF, n = 77), deciduous broadleaf forests (DBF, n = 26,944), shrublands (SHR, n = 1,599), grasslands (GRA, n = 11,833), croplands (CRP, n = 3,409) and vine (n = 637). To better compare the PLSR with RTMs for leaf traits retrieval in the future, we selected four important leaf traits in the compiled dataset and standardized them to the same units (Table S2): total chlorophyll content (Chla+b, $\mu g/cm^2$), total carotenoid content (Ccar, $\mu g/cm^2$), equivalent water thickness (EWT, g/m^2; a.k.a., leaf water content), and leaf mass per area (LMA; g/m^2). This assembled dataset included 6,840 leaf samples

for Chla+b, 4,233 leaf samples for Ccar, 3,581 leaf samples for EWT, and 45,417 leaf samples for LMA. The leaf spectra in the compiled dataset were measured by a variety of instruments such as ASD FieldSpec 3/4/Pro (Malvern Analytical Inc.), SVC HR-1024i full-spectrum spectroradiometer (Spectra Vista Corporation (SVC), Poughkeepsie, NY, USA) and Spectral Evolution PSR-3500 full-range spectrometer (Spectral Evolution, Lawrence, MA, USA), etc. This variability in instruments could affect the transferability of the retrieval methods. Since the spectral sampling interval varies among different spectroradiometers, we resampled leaf spectral data to 10 nm intervals using the full width half maximum (FWHM) resampling method (Adjorlolo *et al.*, 2013), and selected wavelength from 450 nm to 2400 nm for PLSR modeling. In addition, we utilized records in the compiled dataset which have seasonal measurements to investigate the transferability of PLSR over time. A subset of the compiled dataset that had Chla+b, Ccar and LMA measurements and the associated leaf spectral measurements were used to investigate the transferability of the Chla+b, Ccar and LMA model's transferability (Table S1).

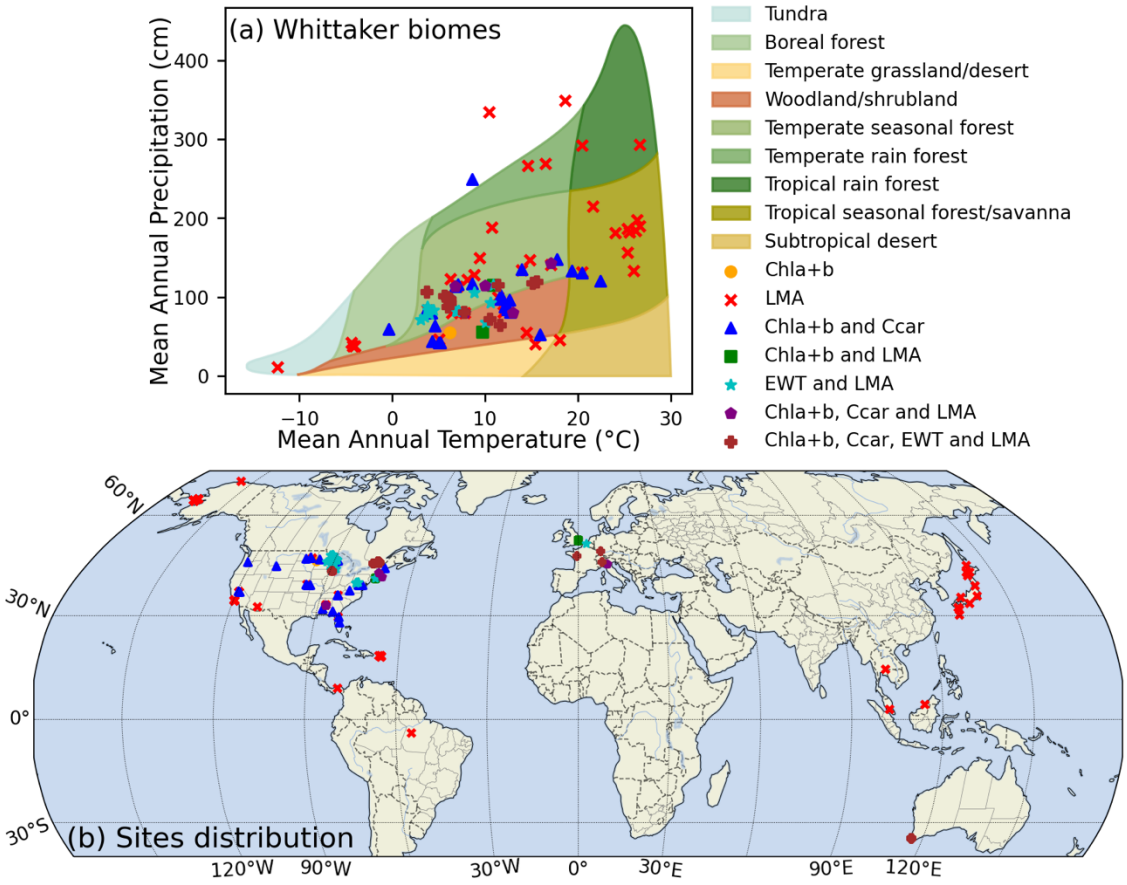

Fig. 1 The distribution of leaf samples in (a) climate zones (Whittaker, 1970) and (b) geographic locations. The orange circle means that the sites only have Chla+b measurements; the red "x" means that the sites only have LMA measurements; the blue triangle refers to the sites with Chla+b and Ccar measurements; the green square refers to the sites with Chla+b and LMA measurements; the cyan star refers to the sites with EWT and LMA measurements; the purple pentagon represents the sites with Chla+b, Ccar and LMA measurements and the filled brown "plus" represents the sites with all the selected leaf traits in this study.

2.2 Partial least-squares regression

PLSR is a linear non-parametric approach that iteratively transforms predictor and response variables to find latent vectors and subsequently produces calibration factors and a linear model. PLSR techniques achieve computational efficiency by maximizing the

covariance between independent and dependent variables while simultaneously maintaining the constraint of being orthogonal to the previously determined factors (Wold *et al.*, 1984; Singh *et al.*, 2015). This makes PLSR especially well-suited to high-dimensional and collinear spectral data. PLSR provides directly interpretable beta coefficients that can be tied to known absorption features. With the leaf spectroscopy and leaf traits, we can express the PLSR as the following equations (Ehsani *et al.*, 1999; Fu *et al.*, 2020):

$$y = \sum_{i=1}^{p} \alpha_i \cdot lv_i, \quad (i = 1, 2, 3, \dots, p) \tag{1}$$

$$lv_i = \sum_{j=1}^{m} \lambda_i \cdot X_j, \quad (j = 1, 2, 3, \dots, m) \tag{2}$$

where *X* and *y* refer to the leaf spectra and leaf traits (e.g., Chla+b, Ccar, EWT or LMA), respectively; *lv* represents the latent vectors calculated from the original leaf reflectance; *p* is the number of latent vectors; m is the number of reflectance wavebands; α represents the regression coefficients. λ represents the eigenvector. In this study, different model validation strategies were used to build PLSR models (Section 2.3). PLSR first reduces the leaf spectra with large collinearity into several orthogonal variables and then finds a linear regression between the orthogonal variables and leaf traits.

2.3 Evaluate the transferability of PLSR

We examined the transferability of PLSR across three dimensions, including site (spatial location), PFT, and time (day of year, DOY) with three sets of experiments with PLSR (Fig. 2).

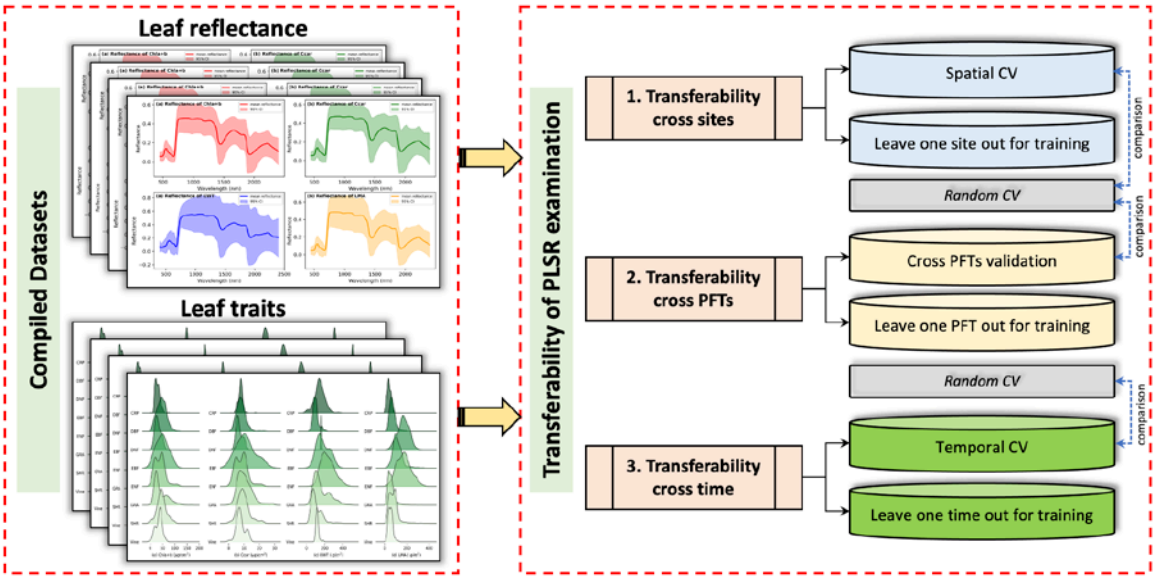

Fig.2. The framework of this study for testing the transferability of PLSR modeling across sites, PFTs and time.

We applied a similar PLSR modeling method with the previous studies (Dechant *et al.*, 2017; Yan *et al.*, 2021), in which the standard PLSR modeling was integrated with a repeated double cross-validation (rdCV) method designed with two (outer and inner) cross-validation loops that can significantly reduce the model bias introduced by data partitioning and result in a stable model (Filzmoser *et al.*, 2009). In the outer CV loop, we first partitioned the entire dataset into k folds and repeatedly used k-1 folds as the calibration set and the remaining fold as the validation set. Within each calibration set, we further randomly divided the data into 70% and 30% splits, repeating this process 100 times for model training (inner CV loop). In each outer CV loop, we calculated the average coefficients and the Variable Importance in Projection (VIP) metric (Wold et al., 2001) across the 100 models resulting from the inner loops. Then the model prediction performance and uncertainties were subsequently assessed using the validation set. Thus by the end of the rdCV, we have k models generated and the final model was acquired by taking the mean of these models.

As a baseline for cross-site and cross-PFT transferability tests, we developed random cross validation. We first fit a preliminary PLSR model for each trait using the random 10-fold CV. This helps to decide the optimal numbers count of PLSR components (up to maximum number of input spectra bands) to be used in the final models by minimizing the Prediction Residual Error Sum of Squares (PRESS). Next, we randomly divided the entire data into 10 folds and repeatedly used 9 folds as the calibration set and the remaining fold as the validation set. Within each iteration, we perform rdCV as explained in the previous context.

For Cross-site modeling, two PLSR modeling analyses were utilized: spatial CV, and leave-one-site-out (LOO) for training CV (Valavi *et al.*, 2019; Meyer *et al.*, 2019; Ploton *et al.*, 2020). (1) In spatial CV, we initially organized all the data into two latitude and longitude rectangular blocks according to their geographic locations (Uieda, 2018), which helped minimize most of the potential spatial autocorrelation between data (Fig. S21); these blocks were subsequently partitioned into 10 subsets and then adopted the spatial 10-fold CV to fit a preliminary PLSR model to determine the optimal numbers of component of spatial PLSR modeling by minimizing PRESS. We then repeatedly utilized 9 subsets for calibration while keeping one subset as the validation set and also employed rdCV for each iteration. The objective of spatial CV modeling is to assess model performance in spatial extrapolation and evaluate whether the spatial autocorrelation has an impact on PLSR performance compared to random CV; (2) For LOO training, the model was trained with data from one site and tested against all other sites, this procedure was repeated once for each site to evaluate the transferability of PLSR among sites. Additionally, we investigated the impact of varying the number of sites utilized for PLSR training on prediction accuracy using a procedure whereby we iteratively increased the number of sites used for training. Subsequently, we calculated CV statistics for every factorial combination of training and

testing sites, and then we evaluated the average and standard deviation of these CV statistics as a function of the number of training sites.

Cross-PFT modeling entailed splitting the full dataset into 5 subsets according to their PFT. Similarly, we first adopted PRESS to determine the optimal count of PLSR components. Next, we iteratively used 4 subsets as calibration sets and one subset as the validation set. Then we performed the rdCV. The objective of cross-PFT modeling is to assess model performance on PFTs extrapolation compared to random CV; Moreover, we performed the analysis on individual PFTs, we left one PFT in the dataset out for model training and tested it against all other PFTs, and other PFTs for validation to evaluate the transferability of PLSR among PFTs. Also, as with sites, we used an iterative procedure to examine how across-PFT transferability changed with the increasing number of PFTs in the training data.

For cross-time modeling, we first used 3 datasets (Datasets ID 3, 4 and 8 (Table S1)) in our compiled dataset that are located in temperate northern hemisphere and featuring seasonal measurements of both leaf traits and reflectance shared the same geographic location and belong to the same PFT (DBF) to investigate the ability of PLSR for temporal extrapolation. This selection was made to rigorously assess the ability of PLSR for temporal extrapolation. Datasets ID 3 and 4 were used to evaluate the transferability of Chla+b and Ccar models and datasets ID 3,4 and 8 for the LMA model. We built PLSR models respectively for each dataset with seasonal measurements and validated and compared the performance using both random and temporal 5-fold CV methods. For temporal 5-fold CV, we evenly split the extracted subsets into 5 measurement time windows and iteratively trained the PLSR model using four time windows as calibration set and validated it against the remaining one window. In each iteration, we then performed the rdCV as described before. We also performed a temporally coarser version of this analysis where we divided the measurement time into early growing season, peak growing

season and post-peak season based on the forest phenology in the region where the dataset is located and tested the transferability between these three seasons. Three strategies were evaluated: (1) training the model with early growing season data and applying it to post-peak season and peak growing season; (2) training the model with peak growing season data and applying it to early growing and post-peak season data; (3) training the model with post-peak season data and applying it to early growing and peak growing season data.

2.4 Statistical Analysis

We used mean values, standard deviations and the range of leaf traits to identify the traits variations across geographic locations and PFTs. We used two-way analysis of variance (ANOVA) to quantify the variations of leaf traits between different sites, PFTs and the variations for the same PFT across sites. The mean and coefficient of variation of leaf reflectance (calculated as the standard deviation divided by mean) of the sample measurements were calculated for each geographic site and PFT to investigate the effects of geolocations and PFTs on leaf spectra. We divided the spectra data into three wavelength domains: 450-750 nm (visible wavelengths, VIS, also includes the red-edge), 750-1300 (near-infrared, NIR), 1300-1800 nm (shortwave infrared 1, SWIR1), and 1800-2400 nm (shortwave infrared 2, SWIR2), to compare and quantify the variations of leaf spectra between sites and PFTs. The performance of PLSR models for estimating leaf traits was evaluated by standard summary statistics including coefficient of determination (R^2), root mean square error (*RMSE*) and normalized root mean square error (*NRMSE*, calculated by the RMSE divided by the range of the estimated leaf traits).

To understand the factors impacting the transferability of PLSR across sites and PFTs, we conducted two analyses. In the first analysis, we grouped all the sites according to their climate zones (Fig. 1a). Then, we quantified the performance of PLSR transformation between sites vs. across climate zones. In the second analysis, we aimed to explore the relationship between the performance of PLSR transformation and spectral diversity. We

utilized two simple spectral diversity metrics, coefficients of variation (Wang *et al.*, 2016, 2018) and pairwise Bray-Curtis (BC) dissimilarity index (Bray & Curtis, 1957; Féret & Asner, 2014), to calculate both alpha (within-community) and beta (across-community) spectral diversity (Schweiger & Laliberté, 2022). We used coefficients of variation as metrics of Alpha spectral diversity, and we used Euclidean distance (Kruse *et al.*, 1993; Fang *et al.*, 2017; Jiang *et al.*, 2021; Wan *et al.*, 2021) — a common spectral similarity metric —to quantify the similarity of alpha spectral diversity between two sites or PFTs. We used the BC dissimilarity index as a metric of Beta spectral diversity to compare the dissimilarity of beta diversity between two sites or PFTs.

Results

3.1 Variations of leaf traits and leaf spectra

3.1.1 Variations of leaf traits

Large variations in leaf traits were found across geographic sites (Fig. S3a-d), PFTs (Fig. S3e-h, Table S3) and through time (Fig. S4-S5). In our compiled dataset, Chla+b ranges from 0.12 to 167.23 μg/cm^2 with a mean value of 35.07 μg/cm^2 and a standard deviation of 19.15 μg/cm^2. Ccar ranges from 0.04 to 28.35 μg/cm^2 with a mean value of 8.35 μg/cm^2 and a standard deviation of 3.03 μg/cm^2. EWT and LMA range from 3.0 to 477.02 g/m^2 and 0.066 to 388.9 g/m^2 with mean ± 1std of 137.37±75.11 g/m^2 and 69.85±35.87 g/m^2, respectively. The distribution of leaf traits showed comparable ranges and variations to the global TRY database (Kattge *et al.*, 2020), which indicates that our data are fairly representative of a substantial portion of global trait variability. (Fig. S6).

For the variations of leaf traits across PFTs, EBF (48.22 ± 23.37 μg/cm^2; mean ± 1std, same in the following text), SHR (45.65±19.73 μg/cm^2) and GRA (38.38±23.35 μg/cm^2) have relatively higher chlorophyll contents, followed by ENF (39.07±20.95 μg/cm^2), DBF (37.77±20.53 μg/cm^2), vine (32.97±13.86 μg/cm^2) and DNF (30.98±11.09 μg/cm^2), and CRP (29.01±9.75 μg/cm^2) have the lowest chlorophyll contents. The variations of

carotenoid content across PFTs show patterns similar to chlorophyll. There are also broad variations in the other two traits, EWT and LMA, across PFTs. For example, ENF has the highest EWT and LMA values (233.19±73.84 g/m^2 and 173.18±63.78 g/m^2, respectively) followed by EBF and DNF. SHR (105.24±62.02 g/m^2) and DBF (93.39±27.84 g/m^2) have lower EWT concentration, vine (53.39±19.95 g/m^2) and CRP (38.77±16.82 g/m^2) show relatively lower in LMA concentration.

For the variations of leaf traits throughout the growing seasons, chlorophyll content and carotenoids pigments will increase rapidly from 16.94 ± 4.9 μg/cm^2, 4.08 ± 0.89 μg/cm^2, respectively at the beginning of the growing season to a stabilized status at the peak growing season, which are 37.65 ± 9.41 μg/cm^2, 7.21 ± 2.16 μg/cm^2 for Chla+b and Ccar, respectively. Followed by declines in the post-peak season with values of 27.44 ± 12.41 μg/cm^2 and 5.65 ± 2.2 μg/cm^2, respectively. Similar to Chla+b and Ccar, LMA will increase rapidly from the beginning of the growing season (61.01 ± 18.27 g/m^2) to the peak growing season (95.56 ± 36.58 g/m^2) and then will increase slowly until leveling off at the end of the peak growing season (114.45 ± 44.34 g/m^2).

The results of ANOVA (Table S4) indicate significant differences in all the selected leaf traits across both sites and PFTs ($p < 0.001$). Differences in the leaf traits of GRA, DBF, CRP, SHR and ENF across sites were also significant ($p < 0.001$). Differences in Chla+b of vine, LMA of EBF and DNF across sites were also significant, but differences in Ccar, EWT and LMA of vines were not significant. Differences in the Ccar of EBF and DNF, and EWT of DNF across sites were not significant ($p > 0.05$).

3.1.2 Variations of leaf spectra

Similar to leaf traits, leaf spectra also show significant variations across geographic sites, PFTs and time (Fig. 3, Fig. S7-S11) over VIS-NIR-SWIR wavelengths, Specifically, the coefficient of variation for leaf spectra across PFTs (Fig. 3 (b), Table S5) is relatively higher for ENF and SHR, but is lower for DNF and CRP, especially spectral domain of

450-750 nm in the VIS band, 1300-1800 nm in the SWIR1 and 1800-2400 nm in the SWIR2 band.

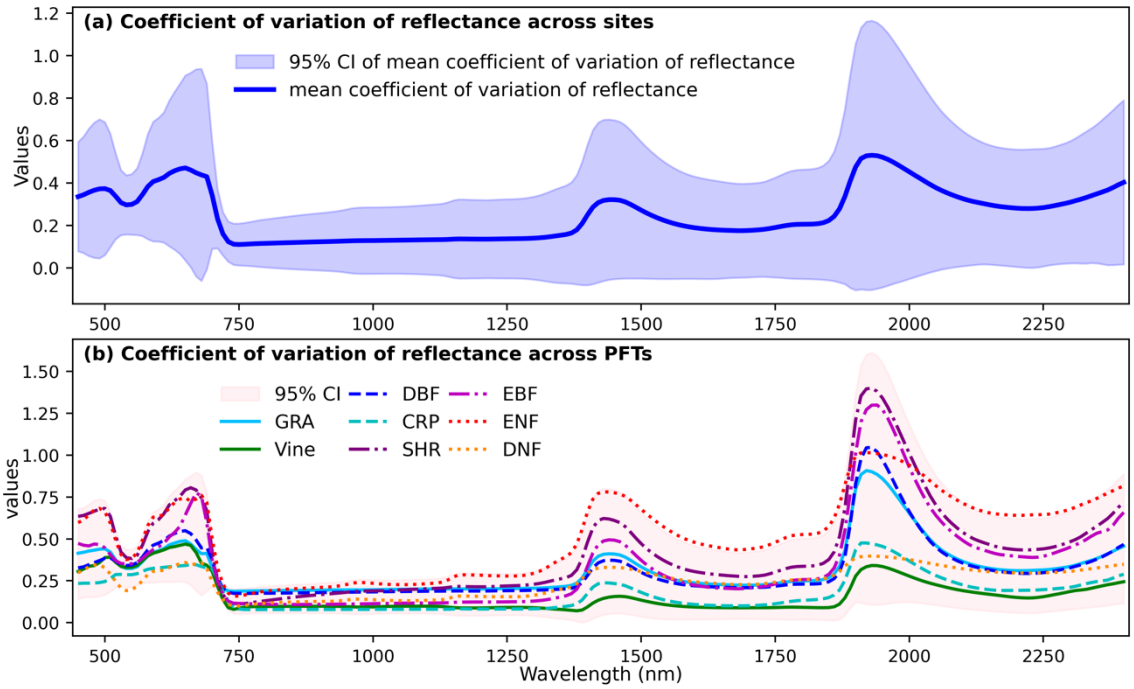

Fig. 3 Coefficient of variation of leaf spectra across geographic sites and PFTs. (a) coefficient of variation of reflectance across geographic sites; (b) coefficient of variation of reflectance across different PFTs.

3.2 PLSR models

PLSR models will be developed across a range of frameworks, with assessments of transferability across space, PFT and time. Results below are therefore provided for each test that was implemented, and Supplemental Tables S6-S9 provide the full range of statistics for each PLSR implementation and test.

3.2.1 Spatial transferability of the PLSR model

Spatial CV reveals that the accuracy of leaf trait estimations using random cross-validation overestimates the likely accuracy of the prediction when applied to samples outside of the spatial domain of the calibration data (Fig. 4). Specifically, the random CV of PLSR (i.e., not informed by spatial location) leads to better prediction of leaf traits

estimation than spatially informed PLSR validation, with 0.49, 0.31, 0.12 and 0.12 higher of R^2 and 18.24%, 13.77%, 3.64% and 3.58% lower of *NRMSE* for Chla+b, Ccar, EWT and LMA predictions, respectively.

The results of 'leave one site out for training' showed that when the trained PLSR is applied to other sites, its performance decreases considerably and its accuracy varies depending on the testing site (Fig. 5). However, as more sites are used to train the model, its performance improves and eventually reaches a stable level (Fig. 6). The transferability of PLSR was not greatly affected by spatial distance between sites (Fig. S12). This implies that factors other than spatial distance between sites contributed to the previously reported overly optimistic performance.

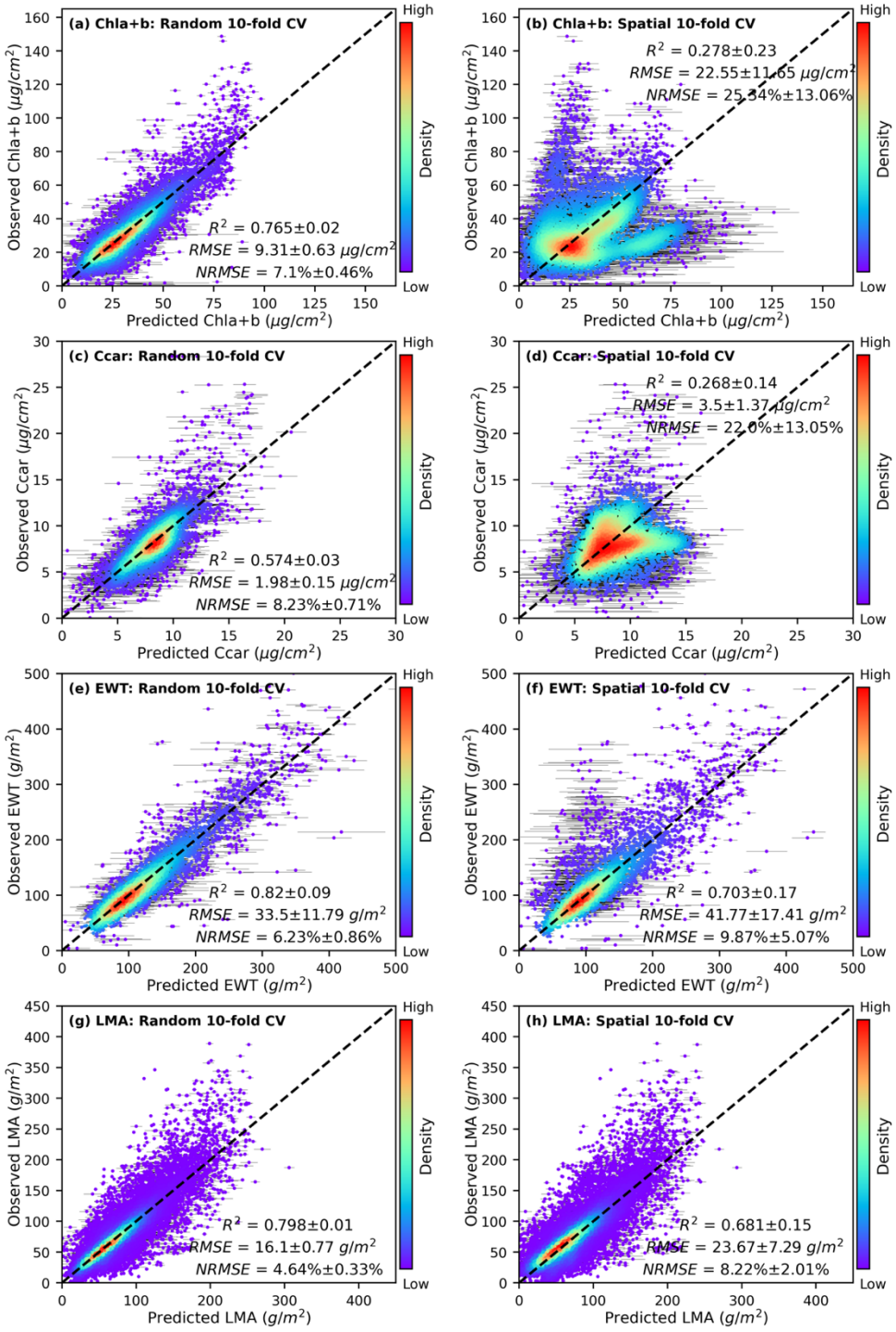

Fig. 4 The relationship between predicted and observed leaf traits. (a), (c), (e), (g) are random 10-fold cross-validation for Chla+b, Ccar, EWT and LMA estimation, respectively; (b), (d), (f), (h) are spatial 10-fold cross-validation for Chla+b, Ccar, EWT and LMA estimation, respectively. Error bars represent the 95% confidence intervals for each

predicted value derived from the ensemble of PLSR models generated through the 100-repetition iterative procedures. The deeper red (purple) color represents the higher (lower) density of data.

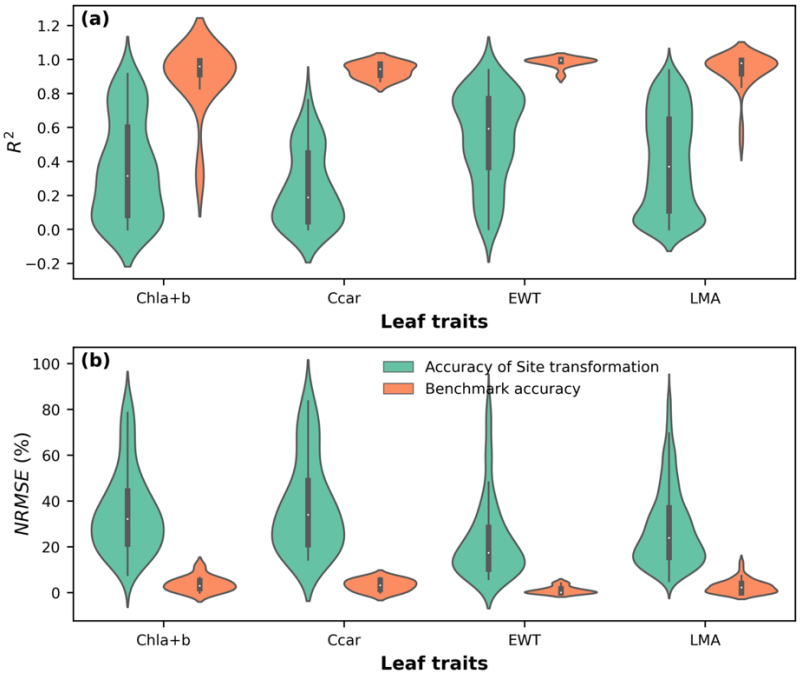

Fig. 5 Performance of the 'leave one site out for training' cross-validation method to test the transferability of PLSR across geographic sites. (a) R^2; (b) *NRMSE*. Orange color is the benchmark accuracy, which means testing model performance using the data from the training site. The green color is the accuracy of applying the trained model from one site to other sites.

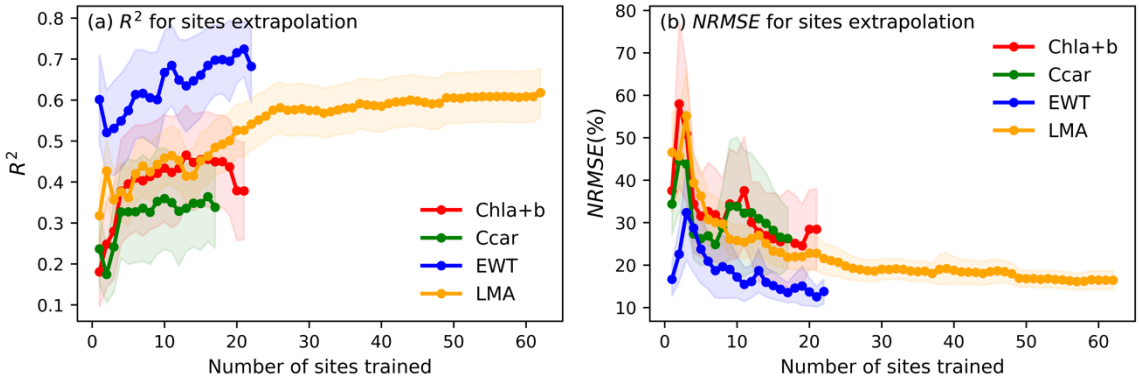

Fig. 6 The relationship between model performance and the number of trained sites.

3.2.2 Transferability of the PLSR model on PFTs

Compared to random cross-validation, the performance of PLSR according to across-PFT validation was much lower (Fig. 7) as well with only R^2 of 0.204±0.17 and *NRMSE* of 28.79±22.53% for Chla+b retrieval; R^2 of 0.152±0.15 and *NRMSE* of 26.53±17.81% for Ccar retrieval; R^2 of 0.572±0.17 and *NRMSE* of 39.35±64% for EWT retrieval and R^2 of 0.473±0.26 and *NRMSE* of 11.46±6.98% for LMA retrieval.

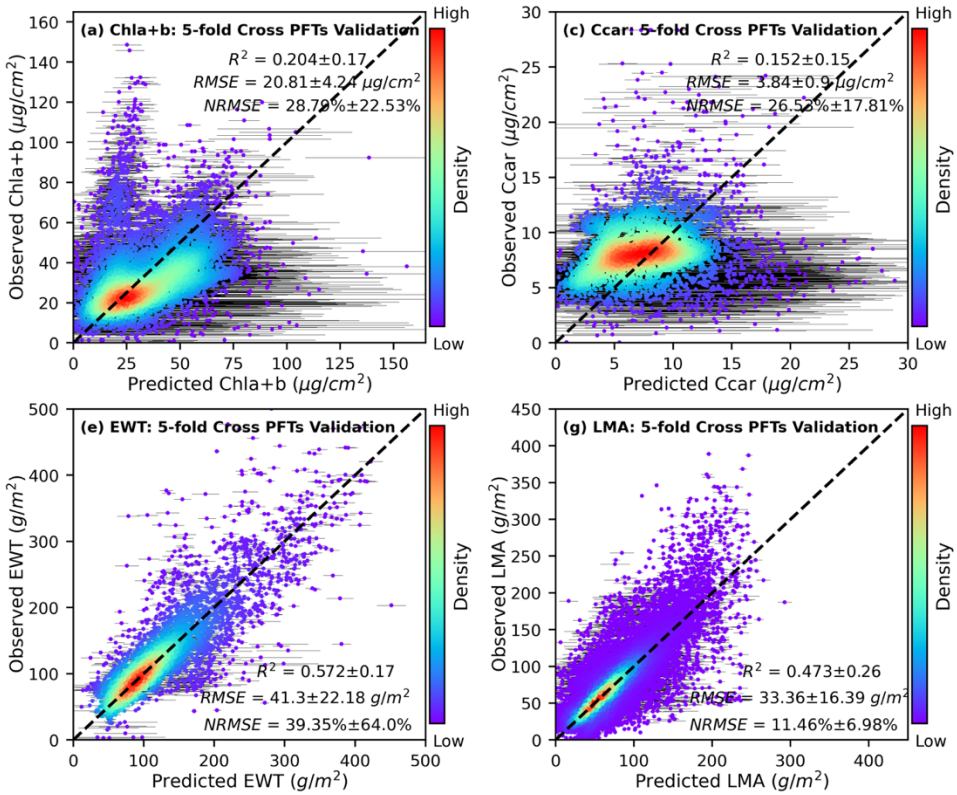

Fig. 7 The relationship between predicted and observed leaf traits by using 5-fold cross-PFT validation method. (a) Chla+b; (b) Ccar; (c) EWT and (d) LMA. Error bars represent the 95% confidence intervals for each predicted value derived from the ensemble of PLSR models generated through the 100-repetition iterative procedures. The deeper orange (purple) color represents the higher (lower) density of data.

On average, PLSR predictions for out-of-sample PFTs were less accurate than in-sample predictions, but the degree of change in accuracy varied depending on the PFT (Fig. 8). The transferability of PLSR across sites also varied by PFT (Fig. 9). For the four

selected leaf traits measurements, PLSR has relatively higher transferability across EBF and CRP sites, followed by GRA, DBF, SHR. And ENF exhibited the lowest transferability across sites. Moreover, as more PFTs are used to train the model, the prediction accuracy for out-of-sample PFTs increased, stabilizing at around 3 PFTs for Chla+b, Ccar, and LMA and 5 PFTs for EWT (Fig. 10).

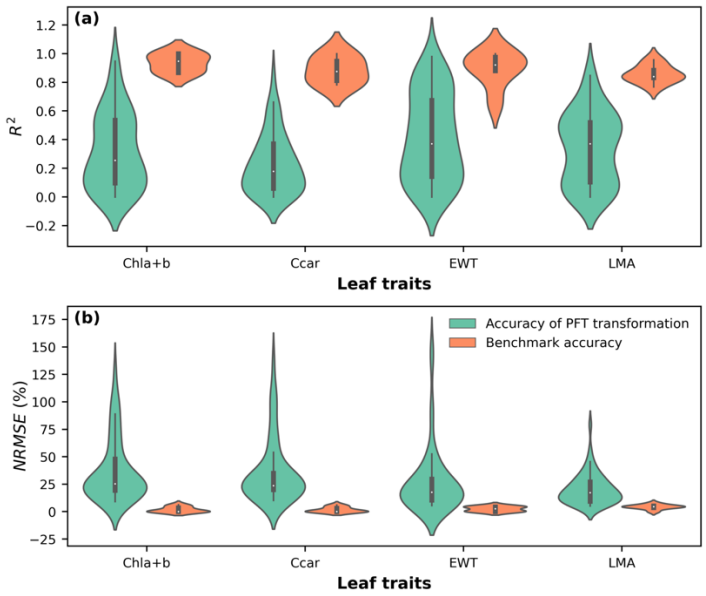

Fig. 8 Performance of the 'leave one PFT out for training' cross-validation method to test the transferability of PLSR across PFTs. (a) R^2; (b) *NRMSE*. Orange color is the benchmark accuracy, which means testing model performance using the data from training PFT. The green color is the accuracy of applying the trained model from one PFT to other PFTs.

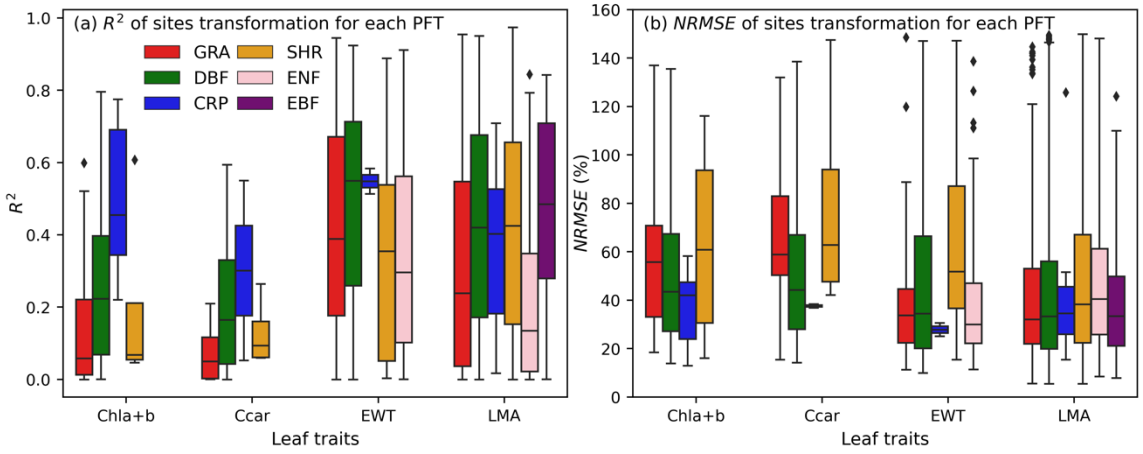

Fig. 9 The accuracy of PLSR across sites for each PFT. (a) R^2; (b) *NRMSE*.

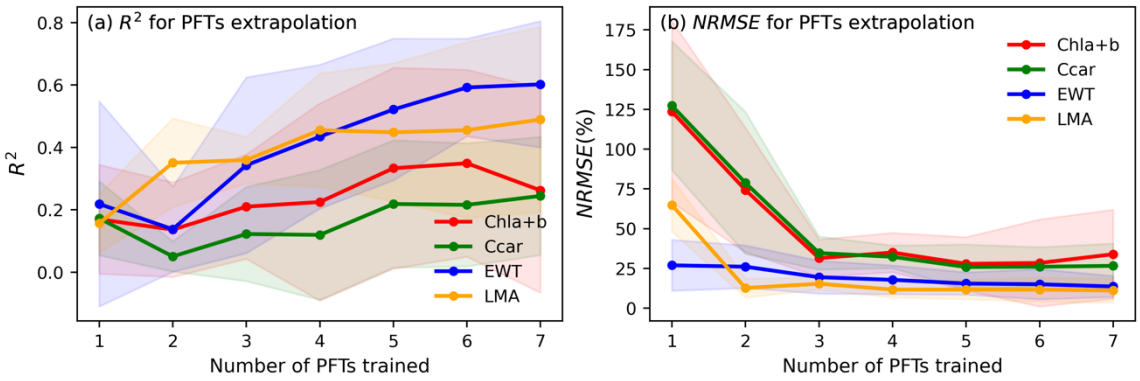

Fig. 10 The relationship between model performance and the number of trained PFTs.

3.2.3 Temporal transferability of the PLSR model

Similar to spatial and PFT aspects, random cross-validation (i.e., not informed by measure time) also lead to better predictions of leaf traits estimation than temporally informed PLSR validation. The random cross-validation method for Chla+b, Ccar and LMA estimation produced R^2 values of 0.75±0.01, 0.598±0.06, 0.735±0.08 and *NRMSE* of 12.9+0.14%, 14.58±1.81%, 12.52±3.35, respectively. On the other hand, the temporal cross-validation method for Chla+b, Ccar and LMA estimation produced lower R^2 values of 0.331±0.01, 0.285±0.04, 0.584±0.13 and higher *NRMSE*s of 24.45±0.71%, 23.06±2.39%, 18.8±6.67%, respectively (Fig. 11). The poor performance of PLSR using the temporal cross-validation method suggests that it is challenging for PLSR to transfer across time.

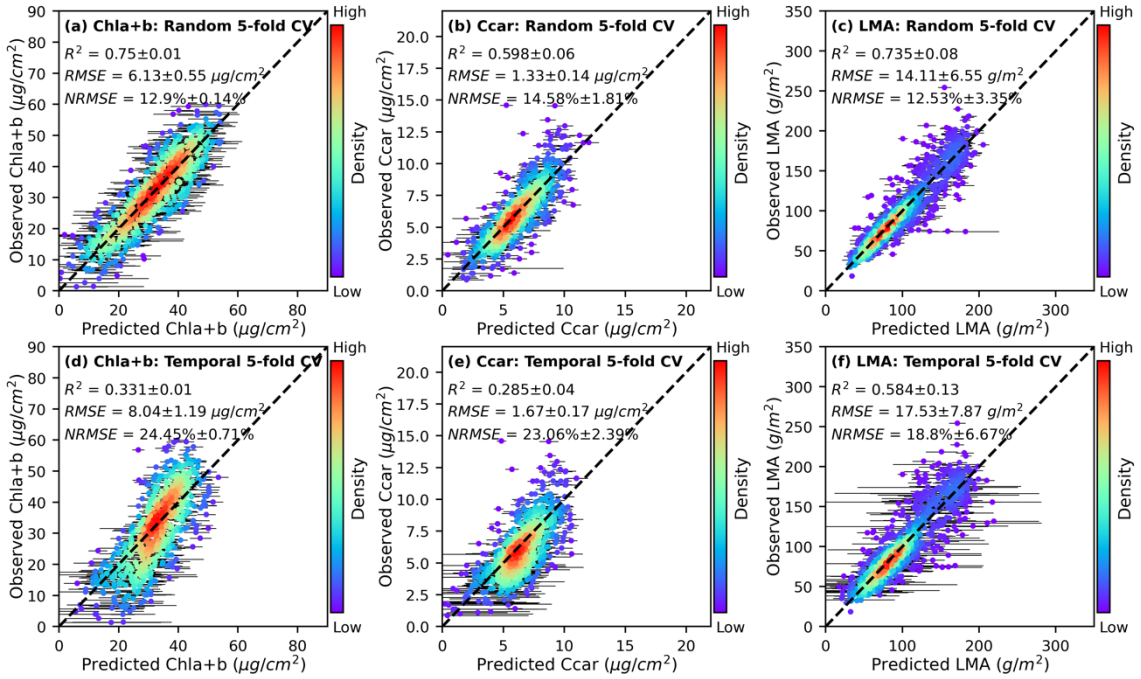

Fig. 11 The relationship between predicted and observed leaf traits. (a), (b) and (c) are random 5-fold cross-validation for Chla+b, Ccar and LMA estimation, respectively; (d), (e) and (f) are temporal 5-fold cross-validation for Chla+b, Ccar and LMA estimation, respectively. Error bars represent the 95% confidence intervals for each predicted value derived from the ensemble of PLSR models generated through the 100-repetition iterative procedures. The deeper orange (purple) color represents the higher (lower) density of data.

The model may systematically overestimate or underestimate the leaf traits when it is applied for cross-seasonal estimation (Fig.12, Fig. S13-S15). For example, For Chla+b and Ccar, when applying the peak growing data trained model to early growing season and post-peak season, leaf traits will be overestimated. Conversely, when applying the early growing season or post-peak season data-trained model to the peak growing season, leaf traits will be underestimated. The inter-transformation between the early growing season and post-peak season models depends on the range of traits. However, the LMA model has a different way of cross-seasonal transformation, as LMA is continuously increasing throughout the growing season. LMA will be underestimated when the LMA model trained

from the early growing season is applied to peak and post-peak growing seasons and vice versa, it will be overestimated. The performance of the model transferring across the seasons depends on the overlap between the data in the training and prediction seasons. For Chla+b and Ccar, models trained from early growing or post-peak season transferred better to peak growing season than vice versa (Fig. 12 a-f, Fig. S13-S14). LMA models outperform Chla+b and Ccar models on cross-seasonal transformation and models trained from and post-peak or peak growing season transferred better to the early growing season than vice versa ((Fig. 12 g-i, Fig. S15)).

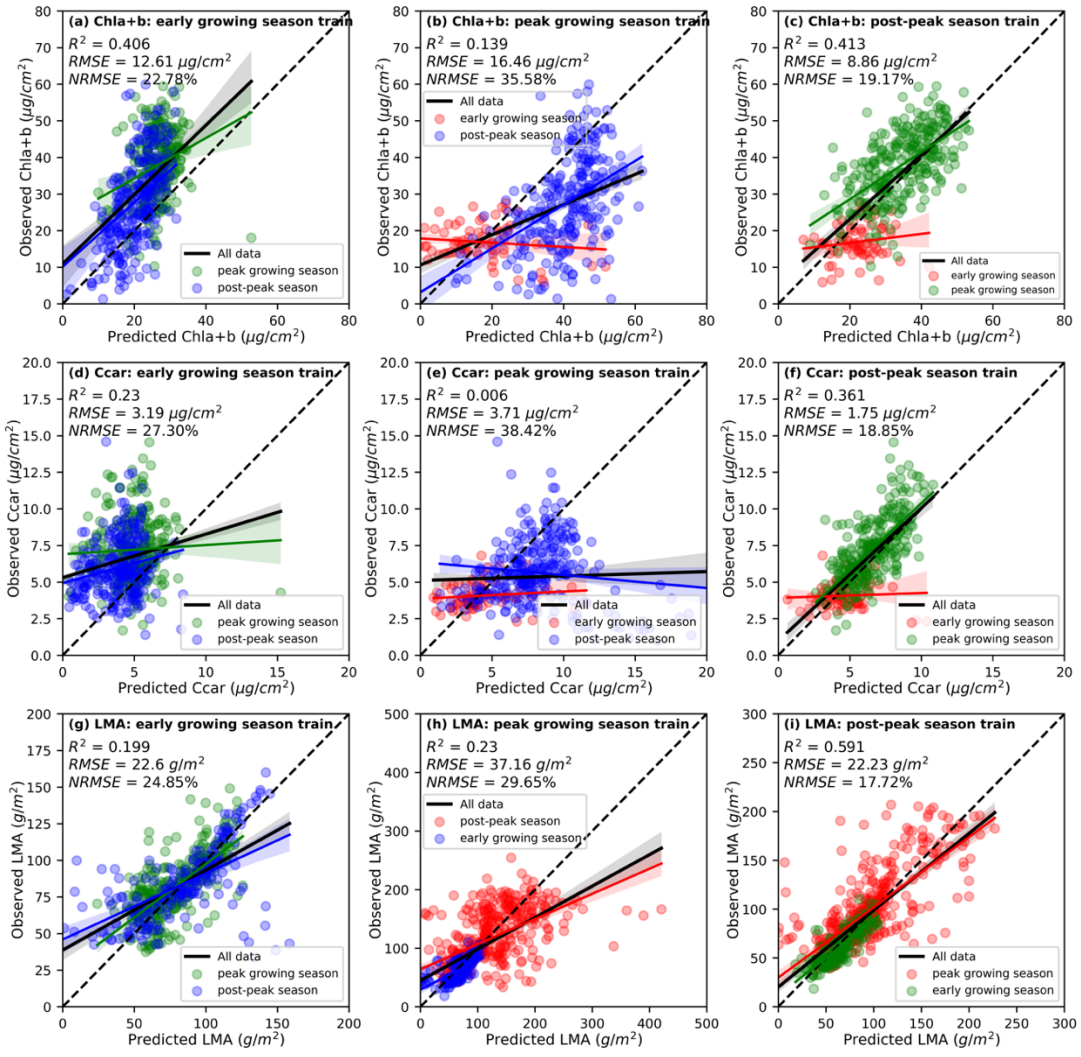

Fig. 12 Evaluation of temporal transferability of the PLSR model. Each row shows PLSR modeling on temporal scales for different leaf traits ((a), (b) and (c) for Chla+b; (d), (e) and

(f) for Ccar; (g), (h) and (i) for LMA). Each column shows different modeling strategies, (a), (d) and (g) show the results of the model trained with early growing season data and applied to peak growing season and post-peak season; (b), (e) and (h) show the results of the model trained with the peak growing season data and applied to the early growing season and post-peak season; (c), (f) and (i) show the results of the model trained with post-peak season data and applied to early growing season and peak growing season, respectively.

3.3 Factors influencing the transferability of PLSR

We found no obvious influence of climate variables on the transferability of PLSR models for trait prediction (Fig.13). Models trained in climate zones of woodland/shrubland, tropical seasonal forest/savanna and boreal forest were more transferable to the sites in the same climate zones, but the climate zone of Temperate seasonal forest was the opposite. Alpha and beta spectral diversity exhibited positive relationships in which greater similarity of a spectral diversity metric yielded greater PLSR transferability. A higher similarity of spectral diversity among sites or PFTs is associated with the higher transferability of PLSR across geographic sites and PFTs (Fig.14).

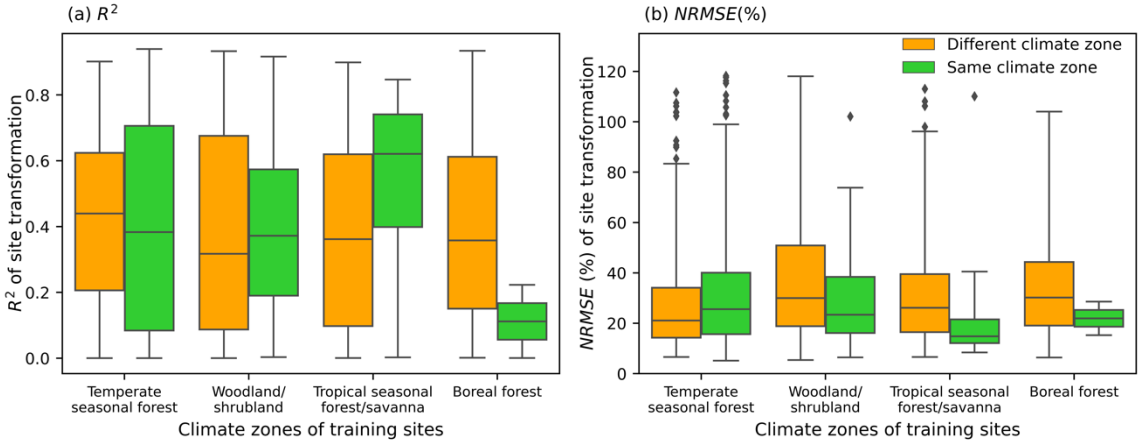

Fig. 13 Climate variables to explain the transferability of PLSR. (a) and (b) refer to R^2 and NRMSE for PLSR transfer across climate zones, respectively.

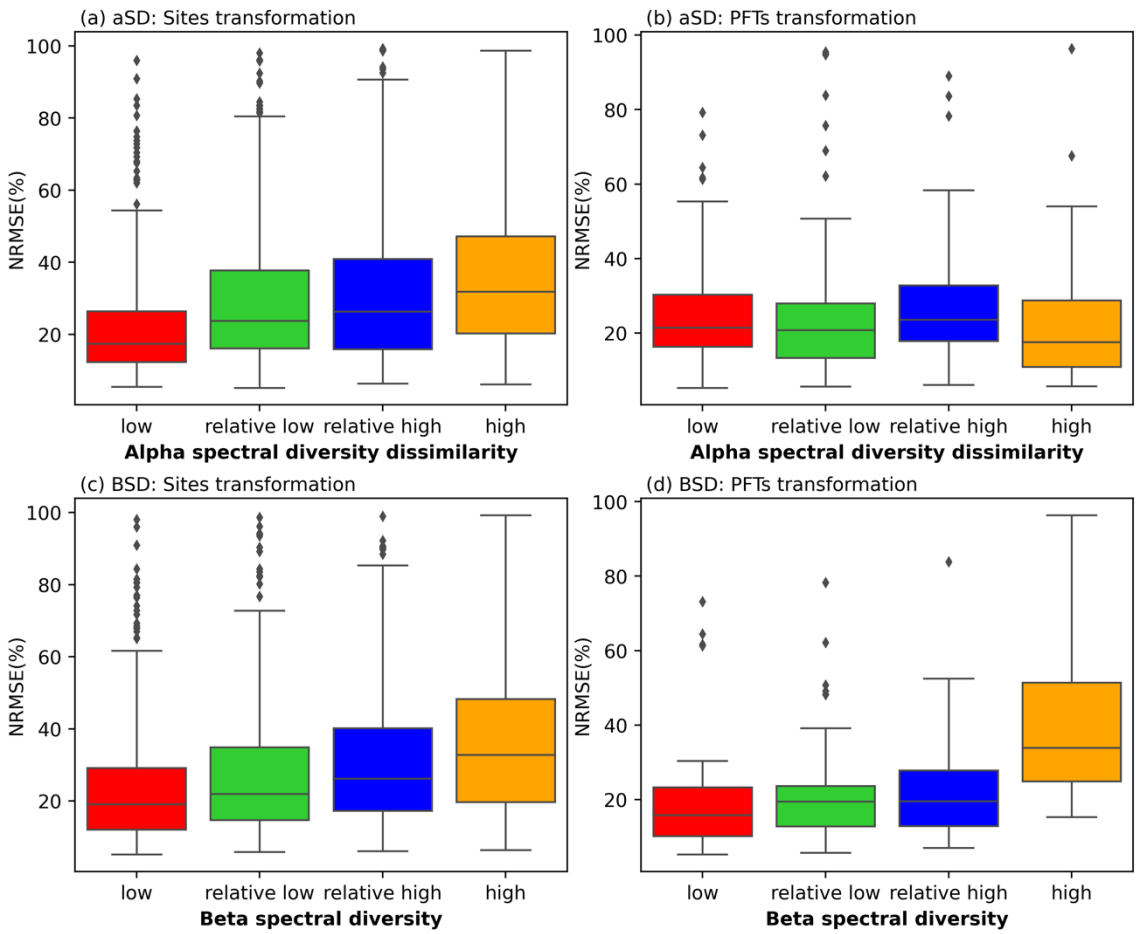

Fig. 14 Alpha and beta spectral diversity to explain the transferability of PLSR. (a) and (b) are the relationships between alpha spectral diversity (aSD) and PLSR transferability across sites and PFTs, respectively. (c) and (d) are the relationships between beta spectral diversity (BSD) and PLSR transferability across sites and PFTs, respectively.

Discussion

In this study, we first compiled a large dataset with common leaf traits and the corresponding leaf spectra spanning a wide range of climate zones and PFTs. We found that both leaf traits and leaf spectra show large variations across sites, PFTs, and phenological stages throughout the growing season (Fig. 3, Fig. S3-S5, S7- S11, Table S3), and the distribution of leaf traits in our compiled dataset showed comparable ranges and variations to the global TRY database (Kattge *et al.*, 2020), which indicates that our data are fairly representative of a substantial portion of global trait variability (Fig. S6). We

used this dataset to examine the transferability of leaf traits – leaf spectra relationships based on the PLSR model and different cross-validation methods. As expected, it is generally feasible to estimate leaf traits from the spectral properties of leaves, which is consistent with the previous studies that the combination of leaf spectroscopy and the PLSR model could be widely applied to infer leaf traits in various scales (Asner *et al.*, 2015; Yang *et al.*, 2016; Hill *et al.*, 2019; Nakaji *et al.*, 2019; Serbin *et al.*, 2019c; Fu *et al.*, 2020; Spafford *et al.*, 2021; Jiang *et al.*, 2021; Yan *et al.*, 2021; Chen *et al.*, 2022; Wan *et al.*, 2022). However, we found that the relationship between leaf traits and spectra was influenced by geographic location, PFT, and timing within a growing season, which can result in relatively poor performance of PLSR to infer leaf traits when applied to novel contexts.

Our observation shows that random cross-validation provides better assessments of model performance when applied to new observation results from the sites, temporal, and PFT representativeness in the training data (Meyer *et al.*, 2019; Ploton *et al.*, 2020). The random cross-validation of PLSR showed similar levels of performance for predicting Chla+b, Ccar, EWT and LMA as previous studies (Singh *et al.*, 2015; Féret *et al.*, 2019; Serbin *et al.*, 2019c; Yan *et al.*, 2021; Chen *et al.*, 2022; Cherif *et al.*, 2023). Our finding of limited PLSR transferability across space (Fig. 4) and across PFTs (Fig. 7) agrees with several other recent studies of PLSR transferability across species (Helsen *et al.*, 2021), across sites (Nakaji *et al.*, 2019; Yan *et al.*, 2021). As well as limited PLSR transferability through time (Fig. 11), confirming that models are generally not transferable across phenological stages for a much more limited leaf data set (Yang *et al.*, 2016) and also demonstrated for image spectroscopy (Schiefer *et al.*, 2021; Chlus & Townsend, 2022b). In general, the model will perform poorly if the data in the training samples cannot represent a large portion of the data in the validation samples (Roberts *et al.*, 2017; Kothari *et al.*, 2023), but the degree of change in accuracy varied depending on the testing sites and

PFT (Fig. 5, Fig 8). However, our results clearly show that including more sites and PFTs in the training data improves PLSR accuracy, up to a limit (Fig. 6, 10), presumably because the overlap between the training and prediction components increased with the number of sites of PFTs. We also quantified the PLSR transferability across sites for different PFT and found that evergreen broadleaf forests and croplands have relatively higher transferability across sites, followed by grasslands, deciduous broadleaf forests and shrublands, with evergreen needleleaf forests having the lowest transferability across sites (Fig.9). The poor performance of ENF may be a consequence of the sampling frequencies and the substantial differences in spectrometer measurement of fresh foliage, which was not used as a screening criterion for the analyses here.

We found that models may systematically overestimate or underestimate the leaf traits when it is applied for cross-seasonal estimation (Fig.12, Fig. S13-S15). The degree of overestimation or underestimation varies between different traits, which is aligned with the previous study (Yang *et al.*, 2016). The performance of the model transferring across the seasons depends on the overlap between the data in the training and prediction seasons. For Chla+b and Ccar, models trained from early growing or post-peak season transferred better to peak growing season than vice versa (Fig. 12 a-f, Fig. S13-S14). LMA models outperform Chla+b and Ccar models on cross-seasonal transformation and models trained from post-peak or peak growing season transferred better to the early growing season than vice versa ((Fig. 12 g-i, Fig. S15)). Variations of leaf traits are strongly related to phenology and change during the growing season in the deciduous species, as during different seasons, leaves are at varying stages of development and optimized for different functions. For instance, in the early growing season, leaves are in the developmental stage with their structure not yet finalized, and biochemical precursors for final structure and function are predominant. As the growing season peaks and leaves mature, their structure and biochemistry are optimized for primary functions such as photosynthesis. In the post-peak

558 season, as leaves become senescent, they are often optimized for transferring essential
559 minerals and molecules back to the plant before ultimately shedding. Such that the range
560 of values across seasons may not overlap (McKown *et al.*, 2013; Chen *et al.*, 2022).

561 The VIP metrics which show the relative importance of bands for predicting leaf traits
562 exhibited consistent patterns across the traits and validation strategies (Fig. S16-S18). The
563 VIP values show that visible wavelengths (450–700 nm), and red-edge wavelengths (700–
564 800 nm) were important for predicting all the selected leaf traits in this study. For Chla+b,
565 the wavelength centered at 450 nm, 550 nm and 730 nm in visible and red-edge range
566 exhibited highest VIP values. The VIP patterns for Ccar models closely resembled those
567 of Chla+b, consistent with many other studies (Yang *et al.*, 2016; Wu *et al.*, 2019; Yan *et*
568 *al.*, 2021; Kothari *et al.*, 2023). These findings suggest that the reflectance in the visible
569 and red-edge range is primarily influenced by leaf pigments and leaf structure (Richardson
570 *et al.*, 2002). Additionally, EWT and LMA exhibited consistently high VIP values scores
571 across much of the shortwave infrared wavelengths, likely indicating the strong and
572 widespread impact of LMA and EWT on SWIR reflectance.

573 Many studies have demonstrated that climate gradients can explain some variations in
574 plant traits (Maire *et al.*, 2015; Simpson *et al.*, 2016; Madani *et al.*, 2018; Yang *et al.*, 2019;
575 Huang *et al.*, 2020; Joswig *et al.*, 2021). However, we also found that climatic variability
576 across sample locations did not explain variability in the transferability of PLSR models
577 for estimating traits from spectra (Fig. 13). In general, climatic effects on trait patterns did
578 not have a corresponding effect on the ability to estimate traits empirically from spectra.
579 The transferability of PLSR across different communities (sites or PFTs) was found to be
580 linked with spectral diversity in leaf spectroscopy, which is crucial in capturing plant
581 species composition and diversity across ecosystems (Wang *et al.*, 2018; Peng *et al.*, 2018;
582 Gholizadeh *et al.*, 2020; Rossi *et al.*, 2021; Schweiger & Laliberté, 2022). Our results show
583 that PLSR models were most transferable between sites and PFTs with comparable levels

584 of alpha and beta spectral diversity. Essentially, a higher similarity of spectral diversity
585 among sites or PFTs corresponds to a higher transferability of PLSR across sites and PFTs
586 (Fig.14). In the realm of data-driven statistical analysis, the best practice is to use predictive
587 models strictly for measurements that falling within the range of the data employed during
588 model training. To fulfill this standard, one can estimate the area of applicability (AOA) of
589 predictive models (Meyer & Pebesma, 2021), which offers a perspective on the extent to
590 which a new observation deviates from the data previously used for model calibration. This
591 study comprehensively evaluated the transferability of PLSR models based on validation
592 in which data are withheld from training according to spatial, temporal and PFTs criteria.
593 A global dataset paired leaf traits and leaf spectra was compiled to support the analyses.
594 Our findings may have three major implications. First, the combination of leaf
595 spectroscopy and the PLSR model can provide robust, rapid, accurate and nondestructive
596 estimates of leaf traits when the distribution of training datasets has a large overlap with
597 the testing datasets (Fig.4 (a, c, e, g); Fig. 11 (a-c)). In other words, the data in the training
598 samples must cover the larger space of potential confounding aspects such as temporal,
599 spatial and PFT than the independent data to which the model is applied. Knowing this
600 point can improve our ability to modulate plant physiological processes and ecosystem
601 dynamics.

602 Second, our work provides new insights and guidance for mapping plant traits and
603 understanding the uncertainties of quantifying foliar traits and associated ecosystem
604 functioning at large or even global scale using the current and forthcoming spaceborne
605 imaging spectroscopy missions. It is likely that trait mapping accomplished from these
606 missions will not have globally comprehensive data for training, and thus users will need
607 to be cautious in their analyses of trait maps that capture conditions not represented in the
608 training data. Finally, our analysis from spatial, temporal, and PFT aspects offers guidance
609 for field sampling strategies to support future biodiversity research at large scales. For

example, we should collect samples as broad as possible to increase the coverage of training data across sites, PFTs and time to ensure the performance of the models.

PLSR is capable of inferring multiple leaf traits simultaneously based on leaf spectroscopy, which enables characterizing relationships among multiple traits. Our compiled dataset had insufficient measurements of multiple traits from a single spectra to conduct such analyses. Consequently, we built separate PLSR for each leaf trait. Therefore, more sophisticated techniques are needed to overcome data sparcity (Cherif *et al.*, 2023) and improve model transferability in the future. Moreover, aggregating multiple datasets led to a notable improvement in model performance in our study (Fig. 6, 10), highlighting the importance of integrating diverse data sources for more accurate leaf trait predictions. However, even with the inclusion of all available datasets, our model's accuracy fell short of its maximum potential. This emphasizes the need for more data for further improvement in model accuracy. Collaborative efforts and open access to diverse datasets are essential for developing more robust models and effectively addressing complex scientific challenges on leaf trait estimations (e.g., through platforms like Ecosis). Furthermore, as we compiled this dataset from various sources such as the EcoSIS database and other publications, it's important to note that the inconsistencies in sampling protocols and pre-processing methods may also contribute to the variations of leaf spectral data and leaf traits which will further impact the subsequent analyses. However, given the limited available information, we only assessed sensor uncertainties within a single dataset (Dataset ID 23, Table S1) from our compiled dataset, which included ASD FieldSpec 3, PSR 3500+, and SVC HR-1024i measurements. We ensured consistency by selecting data with identical location, PFTs, and time, and conducted cross-sensor validation. This involved training models on two sensors and applying the trained models to the remaining sensor. The results (Fig. S19) demonstrated promising accuracy, with R^2 values ranging from 0.726 to 0.926 and NRMSE values spanning from 4.57% to 9.83%. Therefore, in this study, we

disregarded the effects of sensors and focused solely on spatial, PFT-related, and temporal analyses. Additionally, the imbalance of sample representations across various PFTs may introduce additional uncertainties in the PLSR modeling process. To verify this issue, we utilized a Bootstrap approach to equalize the sample sizes among different PFTs, the results (Fig. S20) showed a very similar accuracy with cross PFTs validation (Fig. 7) and did not alter the primary conclusion.

Conclusions

In this study, we compiled a global dataset including leaf spectra paired with measurements of leaf traits that are commonly estimated from spectra. We demonstrate that the patterns of leaf traits and leaf spectra are highly variable across sites, PFTs and phenological stages. Leaf spectroscopy and PLSR modeling are highly capable of quantifying leaf traits given sufficiently comprehensive training data. However, the model performance will significantly decline when extrapolating to novel contexts. We found that the transferability of PLSR was strongly related to spectral diversity among sites or PFTs (i.e., better performance and higher spectral similarity). Moreover, our results confirmed that the current widely-used random cross-validation method might result in overoptimistic model performance and hence provides flawed estimates for assessing the model performance. This work is relevant to regional or even global-scale mapping of plant traits from airborne or satellite hyperspectral sensors and indicates the necessity for comprehensive training data from imaging sensors to ensure robust model performance across vegetation types. Future field sampling strategies should be designed with these considerations in mind.

Data and code availability

All the code of PLSR modeling and the compiled dataset are publicly available GitHub (https://github.com/UW-GCRL/PLSR_trait_models_evaluation). The original dataset can

be found through EcoSIS Spectral Library (https://ecosis.org/) and the cited literature list in Table S1.

Declaration of Competing Interest

The authors declare that they have no known competing financial interests or personal relationships that could have appeared to influence the work reported in this paper.

Acknowledgments

This study is supported by the National Aeronautics and Space Administration (NASA) through Remote Sensing Theory and Terrestrial Ecology programs 80NSSC21K0568 and 80NSSC21K1702. M.C. also acknowledges support from a McIntire–Stennis grant (1027576) from the National Institute of Food and Agriculture (NIFA), United States Department of Agriculture (USDA). A.N.S acknowledges support from NASA New Investigator Program / Terrestrial Ecology (solicitation NNH20ZDA001N-NIP; proposal 20-NIP20-0134). P.T. acknowledges support from NSF Macrosystems Biology and NEON-Enabled Science grants DEB-1638720 and NSF Biology Integration Institute award DBI-2021898. We acknowledge high-performance computing support from the UW-Madison Center for High Throughput Computing (CHTC) in the Department of Computer Sciences. The CHTC is supported by UW-Madison, the Advanced Computing Initiative, the Wisconsin Alumni Research Foundation, the Wisconsin Institutes for Discovery, and the National Science Foundation, and is an active member of the OSG Consortium, which is supported by the National Science Foundation and the U.S. Department of Energy's Office of Science.

Author contributions:

FJ, FL, and MC designed the project with the leaf traits and leaf spectra data from XY, PAT, and TN. FJ processed the data, carried out the analysis, and wrote the first version of the manuscript. DH, ANS, XY, PAT, HD, TN, KRK, HL, ML, and MC revised the manuscript and contributed to the final version.

ORCID

Min Chen: https://orcid.org/0000-0001-6311-7124

Hamid Dashti: https://orcid.org/0000-0001-9397-3458

Dalei Hao: https://orcid.org/0000-0003-3497-9774

Fujiang Ji: https://orcid.org/0000-0003-4623-7487

Kyle R. Kovach: https://orcid.org/0000-0002-1498-6363

Fa Li: https://orcid.org/0000-0002-0625-5587

Meng Luo: https://orcid.org/0009-0009-1158-7226

Haoran Liu: https://orcid.org/0000-0001-5304-5104

Tatsuro Nakaji: https://orcid.org/0000-0002-3161-1539

Alexey N. Shiklomanov: https://orcid.org/0000-0003-4022-5979

Philip A. Townsend: https://orcid.org/0000-0001-7003-8774

Xi Yang: https://orcid.org/0000-0002-5095-6735

References

Adjorlolo C, Mutanga O, Cho MA, Ismail R. **2013**. Spectral resampling based on user-defined inter-band correlation filter: C3 and C4 grass species classification. *International Journal of Applied Earth Observation and Geoinformation* **21**: 535–544.

Albert CH, Thuiller W, Yoccoz NG, Douzet R, Aubert S, Lavorel S. **2010**. A multi-trait approach reveals the structure and the relative importance of intra- vs. interspecific variability in plant traits. *Functional Ecology* **24**: 1192–1201.

Angel Y, Shiklomanov AN. **2022**. Remote Detection and Monitoring of Plant Traits: Theory and Practice. *Annual Plant Reviews Online* **5**: 313–344.

Asner GP, Martin RE. **2008**. Spectral and chemical analysis of tropical forests: Scaling from leaf to canopy levels. *Remote Sensing of Environment* **112**: 3958–3970.

Asner GP, Martin RE, Anderson CB, Knapp DE. **2015**. Quantifying forest canopy traits: Imaging spectroscopy versus field survey. *Remote Sensing of Environment* **158**: 15–27.

Banskota A, Serbin SP, Wynne RH, Thomas VA, Falkowski MJ, Kayastha N, Gastellu-Etchegorry JP, Townsend PA. **2015**. An LUT-Based Inversion of DART Model to Estimate Forest LAI from Hyperspectral Data. *IEEE Journal of Selected Topics in Applied Earth Observations and Remote Sensing* **8**: 3147–3160.

Berger K, Atzberger C, Danner M, D'Urso G, Mauser W, Vuolo F, Hank T. **2018**. Evaluation of the PROSAIL Model Capabilities for Future Hyperspectral Model Environments: A Review Study. *Remote Sensing 2018, Vol. 10, Page 85* **10**: 85.

Blackburn GA. **2007**. Hyperspectral remote sensing of plant pigments. *Journal of Experimental Botany* **58**: 855–867.

Bray JR, Curtis JT. **1957**. An Ordination of the Upland Forest Communities of Southern Wisconsin. *Ecological Monographs* **27**: 325–349.

Breiman L. **2001**. Random Forests. *Machine Learning 2001 45:1* **45**: 5–32.

Burnett AC, Serbin SP, Lamour J, Anderson J, Davidson KJ, Yang D, Rogers A. **2021a**. Seasonal measurements of photosynthesis and leaf traits in scarlet oak - Dataset - EcoSIS Spectral Library.

Burnett AC, Serbin SP, Lamour J, Anderson J, Davidson KJ, Yang D, Rogers A. **2021b**. Seasonal trends in photosynthesis and leaf traits in scarlet oak. *Tree Physiology* **41**: 1413–1424.

Burnett AC, Serbin SP, Rogers A. **2021c**. Leaf and canopy spectroscopy and biochemical data of field-grown Cucurbita pepo under two stresses - Dataset - EcoSIS Spectral Library.

Burnett AC, Serbin SP, Rogers A. **2021d**. Source:sink imbalance detected with leaf- and canopy-level spectroscopy in a field-grown crop. *Plant Cell and Environment* **44**: 2466–2479.

Cavender-Bares J, Gamon JA, Townsend PA. **2020**. Remote Sensing of Plant Biodiversity. *Remote Sensing of Plant Biodiversity*: 581.

Cawse-Nicholson K, Townsend PA, Schimel D, Assiri AM, Blake PL, Buongiorno MF, Campbell P, Carmon N, Casey KA, Correa-Pabón RE, *et al.* 2021. NASA's surface biology and geology designated observable: A perspective on surface imaging algorithms. *Remote Sensing of Environment* **257**: 112349.

Chavana-Bryant C, Gerard FF, Malhi Y, Enquist BJ, Asner GP. **2013**. Leaf Phenology of Amazonian Canopy Trees as Revealed by Spectral and Physiochemical Measurements. *AGUFM* **2013**: B53G-03.

Chavana-Bryant C, Malhi Y, Wu J, Asner GP, Anastasiou A, Enquist BJ, Cosio Caravasi EG, Doughty CE, Saleska SR, Martin RE, *et al.* 2017. Leaf aging of Amazonian canopy trees as revealed by spectral and physiochemical measurements. *New Phytologist* **214**: 1049–1063.

Chen L, Zhang Y, Nunes MH, Stoddart J, Khoury S, Chan AHY, Coomes DA. **2022**. Predicting leaf traits of temperate broadleaf deciduous trees from hyperspectral reflectance: can a general model be applied across a growing season? *Remote Sensing of Environment* **269**: 112767.

Cheng T, Rivard B, Sánchez-Azofeifa A. **2011**. Spectroscopic determination of leaf water content using continuous wavelet analysis. *Remote Sensing of Environment* **115**: 659–670.

Cherif E, Feilhauer H, Berger K, Dao PD, Ewald M, Hank TB, He Y, Kovach KR, Lu B, Townsend PA, *et al.* 2023. From spectra to plant functional traits: Transferable multi-trait models from heterogeneous and sparse data. *Remote Sensing of Environment* **292**: 113580.

Chlus A. **2019**. Leaf level spectra and LMA for a set of trees, forbs, vines and grasses collected in Madison, WI - Dataset - EcoSIS Spectral Library.

Chlus A, Townsend PA. **2022a**. Seasonal fresh leaf spectra and traits, Blackhawk Island, WI - Dataset - EcoSIS Spectral Library.

Chlus A, Townsend PA. **2022b**. Characterizing seasonal variation in foliar biochemistry with airborne imaging spectroscopy. *Remote Sensing of Environment* **275**: 113023.

Clevers JGPW, Gitelson AA. **2013**. Remote estimation of crop and grass chlorophyll and nitrogen content using red-edge bands on Sentinel-2 and -3. *International Journal of Applied Earth Observation and Geoinformation* **23**: 344–351.

Combal B, Baret F, Weiss M, Trubuil A, Macé D, Pragnère A, Myneni R, Knyazikhin Y, Wang L. **2003**. Retrieval of canopy biophysical variables from bidirectional reflectance: Using prior information to solve the ill-posed inverse problem. *Remote Sensing of Environment* **84**: 1–15.

Couture J. **2015**. Common Milkweed Leaf Responses to Water Stress and Elevated Temperature - Dataset - EcoSIS Spectral Library.

Couture J. **2016**. 2014 Cedar Creek ESR Grassland Biodiversity Experiment: Leaf-level Contact Data: Trait Predictions - Dataset - EcoSIS Spectral Library.

Couture JJ, Serbin SP, Townsend PA. **2015**. Elevated temperature and periodic water stress alter growth and quality of common milkweed (Asclepias syriaca) and monarch (Danaus plexippus) larval performance. *Arthropod-Plant Interactions* **9**: 149–161.

Croft H, Chen JM, Zhang Y, Simic A. **2013**. Modelling leaf chlorophyll content in broadleaf and needle leaf canopies from ground, CASI, Landsat TM 5 and MERIS reflectance data. *Remote Sensing of Environment* **133**: 128–140.

Dahlin KM, Asner GP, Field CB. **2013**. Environmental and community controls on plant canopy chemistry in a Mediterranean-type ecosystem. *Proceedings of the National Academy of Sciences of the United States of America* **110**: 6895–6900.

Dechant B, Cuntz M, Vohland M, Schulz E, Doktor D. **2017**. Estimation of photosynthesis traits from leaf reflectance spectra: Correlation to nitrogen content as the dominant mechanism. *Remote Sensing of Environment* **196**: 279–292.

Ehsani MR, Upadhyaya SK, Slaughter D, Shafii S, Pelletier M. **1999**. A NIR Technique for Rapid Determination of Soil Mineral Nitrogen. *Precision Agriculture 1999 1:2* **1**: 219–236.

Ely KS, Burnett AC, Lieberman-Cribbin W, Serbin SP, Rogers A. **2019**. Spectroscopy can predict key leaf traits associated with source-sink balance and carbon-nitrogen status. *Journal of Experimental Botany* **70**: 1789–1799.

Ely KS, Serbin SP, Lieberman-Cribbin W, Rogers A. **2018**. Leaf spectra, structural and biochemical leaf traits of eight crop species - Dataset - EcoSIS Spectral Library.

Fang M, Ju W, Zhan W, Cheng T, Qiu F, Wang J. **2017**. A new spectral similarity water index for the estimation of leaf water content from hyperspectral data of leaves. *Remote Sensing of Environment* **196**: 13–27.

Fassnacht FE, Stenzel S, Gitelson AA. **2015**. Non-destructive estimation of foliar carotenoid content of tree species using merged vegetation indices. *Journal of Plant Physiology* **176**: 210–217.

Féret JB, Asner GP. **2014**. Mapping tropical forest canopy diversity using high-fidelity imaging spectroscopy. *Ecological Applications* **24**: 1289–1296.

Féret JB, Berger K, de Boissieu F, Malenovský Z. **2021**. PROSPECT-PRO for estimating content of nitrogen-containing leaf proteins and other carbon-based constituents. *Remote Sensing of Environment* **252**: 112173.

Feret JB, François C, Asner GP, Gitelson AA, Martin RE, Bidel LPR, Ustin SL, le Maire G, Jacquemoud S. **2008**. PROSPECT-4 and 5: Advances in the leaf optical properties model separating photosynthetic pigments. *Remote Sensing of Environment* **112**: 3030–3043.

Féret JB, Gitelson AA, Noble SD, Jacquemoud S. **2017**. PROSPECT-D: Towards modeling leaf optical properties through a complete lifecycle. *Remote Sensing of Environment* **193**: 204–215.

Féret JB, le Maire G, Jay S, Berveiller D, Bendoula R, Hmimina G, Cheraiet A, Oliveira JC, Ponzoni FJ, Solanki T, *et al.* 2019. Estimating leaf mass per area and equivalent water thickness based on leaf optical properties: Potential and limitations of physical modeling and machine learning. *Remote Sensing of Environment* **231**: 110959.

Filzmoser P, Liebmann B, Varmuza K. **2009**. Repeated double cross validation. *Journal of Chemometrics* **23**: 160–171.

Fu P, Meacham-Hensold K, Guan K, Wu J, Bernacchi C. **2020**. Estimating photosynthetic traits from reflectance spectra: A synthesis of spectral indices, numerical inversion, and partial least square regression. *Plant, Cell & Environment* **43**: 1241–1258.

Ge Y, Atefi A, Zhang H, Miao C, Ramamurthy RK, Sigmon B, Yang J, Schnable JC. **2019**. High-throughput analysis of leaf physiological and chemical traits with VIS-NIR-SWIR spectroscopy: A case study with a maize diversity panel. *Plant Methods* **15**: 1–12.

Gholizadeh H, Gamon JA, Helzer CJ, Cavender-Bares J, Gholizadeh C:, Gamon JA, Helzer CJ, Cavender J. **2020**. Multi-temporal assessment of grassland α- and β-diversity using hyperspectral imaging. *Ecological Applications* **30**: e02145.

Grzybowski M, Wijewardane NK, Atefi A, Ge Y, Schnable JC. **2020**. Leaf spectra and physiological and chemical traits from maize grown under nitrogen stress - Dataset - EcoSIS Spectral Library.

Guanter L, Kaufmann H, Segl K, Foerster S, Rogass C, Chabrillat S, Kuester T, Hollstein A, Rossner G, Chlebek C, *et al.* 2015. The EnMAP Spaceborne Imaging Spectroscopy Mission for Earth Observation. *Remote Sensing 2015, Vol. 7, Pages 8830-8857* **7**: 8830–8857.

Heckmann D, Schlüter U, Weber APM. **2017**. Machine Learning Techniques for Predicting Crop Photosynthetic Capacity from Leaf Reflectance Spectra. *Molecular Plant* **10**: 878–890.

Helsen K, Bassi L, Feilhauer H, Kattenborn T, Matsushima H, Van Cleemput E, Somers B, Honnay O. **2021**. Evaluating different methods for retrieving intraspecific leaf trait variation from hyperspectral leaf reflectance. *Ecological Indicators* **130**: 108111.

Helsen K, Van Cleemput E, Bassi L, Somers B, Honnay O. **2020a**. Leaf spectra of 36 species growing in Rosa rugosa invaded coastal grassland communities in Belgium - Dataset - EcoSIS Spectral Library.

Helsen K, Van Cleemput E, Bassi L, Somers B, Honnay O. **2020b**. Optical traits perform equally well as directly-measured functional traits in explaining the impact of an invasive plant on litter decomposition. *Journal of Ecology* **108**: 2000–2011.

Hill J, Buddenbaum H, Townsend PA. **2019**. Imaging Spectroscopy of Forest Ecosystems: Perspectives for the Use of Space-borne Hyperspectral Earth Observation Systems. *Surveys in Geophysics* **40**: 553–588.

Hornik K, Stinchcombe M, White H. **1989**. Multilayer feedforward networks are universal approximators. *Neural Networks* **2**: 359–366.

Hosgood B, Jacquemoud S, Andreoli G, Verdebout J, Pedrini G, Schmuck G. **1994**. Leaf Optical Properties EXperiment 93 (LOPEX93). *European Commission, Joint Research Centre, Institute for Remote Sensing Applications. Report EUR 16095 EN*: 11.

Huang W, Fonti P, Ræbild A, Larsen JB, Wellendorf H, Hansen JK. **2020**. Variability among Sites and Climate Models Contribute to Uncertain Spruce Growth Projections in Denmark. *Forests 2021, Vol. 12, Page 36* **12**: 36.

Iwasaki A, Ohgi N, Tanii J, Kawashima T, Inada H. **2011**. Hyperspectral Imager Suite (HISUI)-Japanese hyper-multi spectral radiometer. *International Geoscience and Remote Sensing Symposium (IGARSS)*: 1025–1028.

Jacquemoud S, Baret F. **1990**. PROSPECT: A model of leaf optical properties spectra. *Remote Sensing of Environment* **34**: 75–91.

Jacquemoud S, Ustin SL, Verdebout J, Schmuck G, Andreoli G, Hosgood B. **1996**. Estimating leaf biochemistry using the PROSPECT leaf optical properties model. *Remote Sensing of Environment* **56**: 194–202.

Jacquemound S, Bidel L, Francois C, Pavan G. **2003**. ANGERS Leaf Optical Properties Database (2003). *Data Set. Available online: http://ecosis. org (accessed on 5 June 2018)*.

Jay S, Maupas F, Bendoula R, Gorretta N. **2017**. Retrieving LAI, chlorophyll and nitrogen contents in sugar beet crops from multi-angular optical remote sensing: Comparison of vegetation indices and PROSAIL inversion for field phenotyping. *Field Crops Research* **210**: 33–46.

Jiang J, Comar A, Weiss M, Baret F. **2021**. FASPECT: A model of leaf optical properties accounting for the differences between upper and lower faces. *Remote Sensing of Environment* **253**: 112205.

Joswig JS, Wirth C, Schuman MC, Kattge J, Reu B, Wright IJ, Sippel SD, Rüger N, Richter R, Schaepman ME, *et al.* 2021. Climatic and soil factors explain the two-dimensional spectrum of global plant trait variation. *Nature Ecology & Evolution 2021 6:1* **6**: 36–50.

Jung M. **2022**. Predictability and transferability of local biodiversity environment relationships. *PeerJ* **10**: e13872.

Kamoske AG, Dahlin KM, Serbin SP, Stark SC. **2018**. 2018 Talladega National Forest: Leaf level Reflectance Spectra and Foliar Traits - Dataset - EcoSIS Spectral Library.

Kattenborn T, Schiefer F, Schmidtlein S. **2017**. Leaf reflectance plant functional gradient IFGG/KIT - Dataset - EcoSIS Spectral Library.

Kattge J, Bönisch G, Díaz S, Lavorel S, Prentice IC, Leadley P, Tautenhahn S, Werner GDA, Aakala T, Abedi M, *et al.* 2020. TRY plant trait database – enhanced coverage and open access. *Global Change Biology* **26**: 119–188.

Kattge J, Díaz S, Lavorel S, Prentice IC, Leadley P, Bönisch G, Garnier E, Westoby M, Reich PB, Wright IJ, *et al.* 2011. TRY – a global database of plant traits. *Global Change Biology* **17**: 2905–2935.

Kimes DS, Knyazikhin Y, Privette JL, Abuelgasim AA, Gao F. **2009**. Inversion methods for physically-based models. *http://dx.doi.org/10.1080/02757250009532396* **18**: 381–439.

Knyazikhin Y, Martonchik J V., Diner DJ, Myneni RB, Verstraete M, Pinty B, Gobron N. **1998**. Estimation of vegetation canopy leaf area index and fraction of absorbed photosynthetically active radiation from atmosphere-corrected MISR data. *Journal of Geophysical Research: Atmospheres* **103**: 32239–32256.

Kothari S, Beauchamp-Rioux R, Blanchard F, Crofts AL, Girard A, Guilbeault-Mayers X, Hacker PW, Pardo J, Schweiger AK, Demers-Thibeault S, *et al.* 2023. Predicting leaf traits across functional groups using reflectance spectroscopy. *New Phytologist*.

Kothari S, Beauchamp-Rioux R, Cavender-Bares. EL and J. **2022a**. Fresh-leaf CABO spectra from herbarium project - Dataset - EcoSIS Spectral Library.

Kothari S, Beauchamp-Rioux R, Laliberté E, Cavender-Bares J. **2022b**. Reflectance spectroscopy allows rapid, accurate, and non-destructive estimates of functional traits from pressed leaves. *bioRxiv*: 2021.04.21.440856.

Kothari S, Erding M, Cavender-Bares. J. **2022c**. 2018 Cedar Creek pressed leaves - Dataset - EcoSIS Spectral Library.

Kruse FA, Lefkoff AB, Boardman JW, Heidebrecht KB, Shapiro AT, Barloon PJ, Goetz AFH. **1993**. The spectral image processing system (SIPS)—interactive visualization and analysis of imaging spectrometer data. *Remote Sensing of Environment* **44**: 145–163.

Lewis P, Disney M. **2007**. Spectral invariants and scattering across multiple scales from within-leaf to canopy. *Remote Sensing of Environment* **109**: 196–206.

Loizzo R, Daraio M, Guarini R, Longo F, Lorusso R, DIni L, Lopinto E. **2019**. Prisma Mission Status and Perspective. *International Geoscience and Remote Sensing Symposium (IGARSS)*: 4503–4506.

Madani N, Kimball JS, Ballantyne AP, Affleck DLR, Van Bodegom PM, Reich PB, Kattge J, Sala A, Nazeri M, Jones MO, *et al.* 2018. Future global productivity will be affected by plant trait response to climate. *Scientific Reports 2018 8:1* **8**: 1–10.

Maire V, Wright IJ, Prentice IC, Batjes NH, Bhaskar R, van Bodegom PM, Cornwell WK, Ellsworth D, Niinemets Ü, Ordonez A, *et al.* 2015. Global effects of soil and climate on leaf photosynthetic traits and rates. *Global Ecology and Biogeography* **24**: 706–717.

Martin ME, Plourde LC, Ollinger S V., Smith ML, McNeil BE. **2008**. A generalizable method for remote sensing of canopy nitrogen across a wide range of forest ecosystems. *Remote Sensing of Environment* **112**: 3511–3519.

McKown AD, Guy RD, Azam MS, Drewes EC, Quamme LK. **2013**. Seasonality and phenology alter functional leaf traits. *Oecologia* **172**: 653–665.

Meerdink S. **2016**. Fresh Leaf VSWIR Spectra to Estimate Leaf Traits for California Ecosystems - Dataset - EcoSIS Spectral Library.

Meerdink SK, Roberts DA, King JY, Roth KL, Dennison PE, Amaral CH, Hook SJ. **2016**. Linking seasonal foliar traits to VSWIR-TIR spectroscopy across California ecosystems. *Remote Sensing of Environment* **186**: 322–338.

Messier J, McGill BJ, Enquist BJ, Lechowicz MJ. **2017**. Trait variation and integration across scales: is the leaf economic spectrum present at local scales? *Ecography* **40**: 685–697.

Messier J, McGill BJ, Lechowicz MJ. **2010**. How do traits vary across ecological scales? A case for trait-based ecology. *Ecology Letters* **13**: 838–848.

Meyer H, Pebesma E. **2021**. Predicting into unknown space? Estimating the area of applicability of spatial prediction models. *Methods in Ecology and Evolution* **12**: 1620–1633.

Meyer H, Reudenbach C, Wöllauer S, Nauss T. **2019**. Importance of spatial predictor variable selection in machine learning applications – Moving from data reproduction to spatial prediction. *Ecological Modelling* **411**: 108815.

Moharana S, Dutta S. **2016**. Spatial variability of chlorophyll and nitrogen content of rice from hyperspectral imagery. *ISPRS Journal of Photogrammetry and Remote Sensing* **122**: 17–29.

Nakaji T, Oguma H, Nakamura M, Kachina P, Asanok L, Marod D, Aiba M, Kurokawa H, Kosugi Y, Kassim AR, *et al.* 2019. Estimation of six leaf traits of East Asian forest tree species by leaf spectroscopy and partial least square regression. *Remote Sensing of Environment* **233**: 111381.

Nieke J, Rast M. **2018**. Towards the copernicus hyperspectral imaging mission for the environment (CHIME). *International Geoscience and Remote Sensing Symposium (IGARSS)* **2018-July**: 157–159.

Osnas JLD, Lichstein JW, Reich PB, Pacala SW. **2013**. Global leaf trait relationships: Mass, area, and the leaf economics spectrum. *Science* **340**: 741–744.

Peng Y, Fan M, Song J, Cui T, Li R. **2018**. Assessment of plant species diversity based on hyperspectral indices at a fine scale. *Scientific Reports 2018 8:1* **8**: 1–11.

Pereira HM, Ferrier S, Walters M, Geller GN, Jongman RHG, Scholes RJ, Bruford MW, Brummitt N, Butchart SHM, Cardoso AC, *et al.* 2013. Essential biodiversity variables. *Science* **339**: 277–278.

Ploton P, Mortier F, Réjou-Méchain M, Barbier N, Picard N, Rossi V, Dormann C, Cornu G, Viennois G, Bayol N, *et al.* 2020. Spatial validation reveals poor predictive performance of large-scale ecological mapping models. *Nature Communications 2020 11:1* **11**: 1–11.

Poorter H, Niinemets Ü, Poorter L, Wright IJ, Villar R. **2009**. Causes and consequences of variation in leaf mass per area (LMA): a meta-analysis. *New Phytologist* **182**: 565–588.

Puglielli G, Crescente MF, Frattaroli AR, Gratani L. **2015**. Leaf Mass Per Area (LMA) as a Possible Predictor of Adaptive Strategies in Two Species of Sesleria (Poaceae): Analysis of

Morphological, Anatomical and Physiological Leaf Traits. *https://doi.org/10.5735/085.052.0201* **52**: 135–143.

Rasmussen CE. **2004**. Gaussian Processes in machine learning. *Lecture Notes in Computer Science (including subseries Lecture Notes in Artificial Intelligence and Lecture Notes in Bioinformatics)* **3176**: 63–71.

Regos A, Gonçalves J, Arenas-Castro S, Alcaraz-Segura D, Guisan A, Honrado JP. **2022**. Mainstreaming remotely sensed ecosystem functioning in ecological niche models. *Remote Sensing in Ecology and Conservation* **8**: 431–447.

Richardson AD, Duigan SP, Berlyn GP. **2002**. An evaluation of noninvasive methods to estimate foliar chlorophyll content. *New Phytologist* **153**: 185–194.

Roberts DR, Bahn V, Ciuti S, Boyce MS, Elith J, Guillera-Arroita G, Hauenstein S, Lahoz-Monfort JJ, Schröder B, Thuiller W, *et al.* 2017. Cross-validation strategies for data with temporal, spatial, hierarchical, or phylogenetic structure. *Ecography* **40**: 913–929.

Rossi C, Kneubühler M, Schütz M, Schaepman ME, Haller RM, Risch AC. **2021**. Remote sensing of spectral diversity: A new methodological approach to account for spatio-temporal dissimilarities between plant communities. *Ecological Indicators* **130**: 108106.

Ruban A V., Berera R, Ilioaia C, Van Stokkum IHM, Kennis JTM, Pascal AA, Van Amerongen H, Robert B, Horton P, Van Grondelle R. **2007**. Identification of a mechanism of photoprotective energy dissipation in higher plants. *Nature 2007 450:7169* **450**: 575–578.

Schiefer F, Schmidtlein S, Kattenborn T. **2021**. The retrieval of plant functional traits from canopy spectra through RTM-inversions and statistical models are both critically affected by plant phenology. *Ecological Indicators* **121**: 107062.

Schweiger AK, Laliberté E. **2022**. Plant beta-diversity across biomes captured by imaging spectroscopy. *Nature Communications 2022 13:1* **13**: 1–7.

Serbin SP. **2016**. Dried Leaf Spectra to Estimate Leaf Morphology and Biochemistry for Northern Temperate Forests - Dataset - EcoSIS Spectral Library.

Serbin SP, Dillaway DN, Kruger EL, Townsend PA. **2012**. Leaf optical properties reflect variation in photosynthetic metabolism and its sensitivity to temperature. *Journal of Experimental Botany* **63**: 489–502.

Serbin SP, Ely K, Rogers A, Dickman T, Detto M, Wu J, Wolfe B, McDowell N, Grossiord C, Michaletz S, *et al.* 2019a. NGEE Tropics Leaf Spectral Reflectance Measured in Panama Collected February to April 2016 - Dataset - EcoSIS Spectral Library.

Serbin SP, Meng R, Wu J, Ely K. **2019b**. NGEE Tropics GLiHT Puerto Rico Campaign Leaf Spectral Reflectance and Transmittance March 2017 - Dataset - EcoSIS Spectral Library.

Serbin SP, Rogers A. **2016**. NGEE Arctic 2016 Leaf Spectral Reflectance Kougarok Road Watershed Seward Peninsula Alaska - Dataset - EcoSIS Spectral Library.

Serbin SP, Rogers A, Liebig J. **2018**. NGEE Arctic Leaf Spectral Reflectance Utqiagvik (Barrow) Alaska 2013 - Dataset - EcoSIS Spectral Library.

Serbin SP, Singh A, McNeil BE, Kingdon CC, Townsend PA. **2014**. Spectroscopic determination of leaf morphological and biochemical traits for northern temperate and boreal tree species. *Ecological Applications* **24**: 1651–1669.

Serbin SP, Townsend PA. **2014**. NASA FFT Project Leaf Reflectance Morphology and Biochemistry for Northern Temperate Forests - Dataset - EcoSIS Spectral Library.

Serbin SP, Wu J, Ely K. **2021**. NGEE Tropics February 2017 Leaf Spectral Reflectance Measured in Panama at the PA-SLZ Canopy Crane - Dataset - EcoSIS Spectral Library.

Serbin SP, Wu J, Ely KS, Kruger EL, Townsend PA, Meng R, Wolfe BT, Chlus A, Wang Z, Rogers A. **2019c**. From the Arctic to the tropics: multibiome prediction of leaf mass per area using leaf reflectance. *New Phytologist* **224**: 1557–1568.

Serbin SP, Yang D, Hantson W, Ely KS. **2019d**. NGEE Arctic 2019 Leaf Spectral Reflectance Seward Peninsula Alaska - Dataset - EcoSIS Spectral Library.

Serbin SP, Yang D, Meng R, McMahon A, Hantson W, Hayes D, Ely K. **2017**. NGEE Arctic 2017 Leaf Spectral Reflectance Teller Watershed Seward Peninsula Alaska - Dataset - EcoSIS Spectral Library.

Simpson AH, Richardson SJ, Laughlin DC. **2016**. Soil–climate interactions explain variation in foliar, stem, root and reproductive traits across temperate forests. *Global Ecology and Biogeography* **25**: 964–978.

Singh A. **2013**. Productivity and Characterization of Soybean Foliar Traits Under Aphid Pressure - Dataset - EcoSIS Spectral Library.

Singh A, Serbin SP, McNeil BE, Kingdon CC, Townsend PA. **2015**. Imaging spectroscopy algorithms for mapping canopy foliar chemical and morphological traits and their uncertainties. *Ecological Applications* **25**: 2180–2197.

Smola AJ, Schölkopf B. **2004**. A tutorial on support vector regression. *Statistics and Computing 2004 14:3* **14**: 199–222.

Spafford L, le Maire G, MacDougall A, de Boissieu F, Féret JB. **2021**. Spectral subdomains and prior estimation of leaf structure improves PROSPECT inversion on reflectance or transmittance alone. *Remote Sensing of Environment* **252**: 112176.

Stein A, Kreft H. **2015**. Terminology and quantification of environmental heterogeneity in species-richness research. *Biological Reviews* **90**: 815–836.

Streher AS, Torres R da S, Morellato LPC, Silva TSF. **2020**. Accuracy and limitations for spectroscopic prediction of leaf traits in seasonally dry tropical environments. *Remote Sensing of Environment* **244**: 111828.

Sun J, Shi S, Yang J, Du L, Gong W, Chen B, Song S. **2018**. Analyzing the performance of PROSPECT model inversion based on different spectral information for leaf biochemical properties retrieval. *ISPRS Journal of Photogrammetry and Remote Sensing* **135**: 74–83.

Thenkabail PS, Mariotto I, Gumma MK, Middleton EM, Landis DR, Huemmrich KF. **2013**. Selection of hyperspectral narrowbands (hnbs) and composition of hyperspectral twoband vegetation indices (HVIS) for biophysical characterization and discrimination of crop types using

field reflectance and hyperion/EO-1 data. *IEEE Journal of Selected Topics in Applied Earth Observations and Remote Sensing* **6**: 427–439.

Townsend PA, Foster JR, Chastain RA, Currie WS. **2003**. Application of imaging spectroscopy to mapping canopy nitrogen in the forest of the central Appalachian mountains using hyperion and AVIRIS. *IEEE Transactions on Geoscience and Remote Sensing* **41**: 1347–1354.

Uieda L. **2018**. Verde: Processing and gridding spatial data using Green's functions. *Journal of Open Source Software* **3**: 957.

Ustin SL, Gitelson AA, Jacquemoud S, Schaepman M, Asner GP, Gamon JA, Zarco-Tejada P. **2009**. Retrieval of foliar information about plant pigment systems from high resolution spectroscopy. *Remote Sensing of Environment* **113**: S67–S77.

Valavi R, Elith J, Lahoz-Monfort JJ, Guillera-Arroita G. **2019**. blockCV: An r package for generating spatially or environmentally separated folds for k-fold cross-validation of species distribution models. *Methods in Ecology and Evolution* **10**: 225–232.

Verrelst J, Malenovský Z, Van der Tol C, Camps-Valls G, Gastellu-Etchegorry JP, Lewis P, North P, Moreno J. **2019**. Quantifying Vegetation Biophysical Variables from Imaging Spectroscopy Data: A Review on Retrieval Methods. *Surveys in Geophysics* **40**: 589–629.

Verrelst J, Muñoz J, Alonso L, Delegido J, Rivera JP, Camps-Valls G, Moreno J. **2012**. Machine learning regression algorithms for biophysical parameter retrieval: Opportunities for Sentinel-2 and -3. *Remote Sensing of Environment* **118**: 127–139.

Villa P, Bolpagni R, Pinardi M, Tóth VR. **2021a**. Leaf reflectance and tratis of floating and emergent macrophytes - Dataset - EcoSIS Spectral Library.

Villa P, Bolpagni R, Pinardi M, Tóth VR. **2021b**. Leaf reflectance can surrogate foliar economics better than physiological traits across macrophyte species. *Plant Methods* **17**.

Violle C, Navas ML, Vile D, Kazakou E, Fortunel C, Hummel I, Garnier E. **2007**. Let the concept of trait be functional! *Oikos* **116**: 882–892.

Violle C, Reich PB, Pacala SW, Enquist BJ, Kattge J. **2014**. The emergence and promise of functional biogeography. *Proceedings of the National Academy of Sciences* **111**: 13690–13696.

Wan L, Zhang J, Xu Y, Huang Y, Zhou W, Jiang L, He Y, Cen H. **2021**. PROSDM: Applicability of PROSPECT model coupled with spectral derivatives and similarity metrics to retrieve leaf biochemical traits from bidirectional reflectance. *Remote Sensing of Environment* **267**: 112761.

Wan L, Zhou W, He Y, Wanger TC, Cen H. **2022**. Combining transfer learning and hyperspectral reflectance analysis to assess leaf nitrogen concentration across different plant species datasets. *Remote Sensing of Environment* **269**: 112826.

Wang Z. **2019a**. Fresh Leaf Spectra to Estimate Foliar Functional Traits over NEON domains in eastern United States - Dataset - EcoSIS Spectral Library.

Wang Z. **2019b**. Fresh Leaf Spectra to Estimate LMA over NEON domains in eastern United States - Dataset - EcoSIS Spectral Library.

Wang Z. **2022**. Fresh Leaf Spectra to Estimate Foliar Functional Traits across NEON domains - Dataset - EcoSIS Spectral Library.

Wang R, Gamon JA, Cavender-Bares J, Townsend PA, Zygielbaum AI. **2018**. The spatial sensitivity of the spectral diversity–biodiversity relationship: an experimental test in a prairie grassland. *Ecological Applications* **28**: 541–556.

Wang R, Gamon JA, Emmerton CA, Li H, Nestola E, Pastorello GZ, Menzer O. **2016**. Integrated Analysis of Productivity and Biodiversity in a Southern Alberta Prairie. *Remote Sensing 2016, Vol. 8, Page 214* **8**: 214.

Wang S, Guan K, Wang Z, Ainsworth EA, Zheng T, Townsend PA, Liu N, Nafziger E, Masters MD, Li K, *et al.* 2021. Airborne hyperspectral imaging of nitrogen deficiency on crop traits and yield of maize by machine learning and radiative transfer modeling. *International Journal of Applied Earth Observation and Geoinformation* **105**: 102617.

Wang Z, Skidmore AK, Wang T, Darvishzadeh R, Hearne J. **2015**. Applicability of the PROSPECT model for estimating protein and cellulose + lignin in fresh leaves. *Remote Sensing of Environment* **168**: 205–218.

Wessels KJ, van den Bergh F, Scholes RJ. **2012**. Limits to detectability of land degradation by trend analysis of vegetation index data. *Remote Sensing of Environment* **125**: 10–22.

Whittaker RH. **1970**. Communities and ecosystems. *Communities and ecosystems.*

Wold S, Ruhe A, Wold H, Dunn, III WJ. **1984**. The Collinearity Problem in Linear Regression. The Partial Least Squares (PLS) Approach to Generalized Inverses. *SIAM Journal on Scientific and Statistical Computing* **5**: 735–743.

Wright IJ, Reich PB, Westoby M, Ackerly DD, Baruch Z, Bongers F, Cavender-Bares J, Chapin T, Cornellssen JHC, Diemer M, *et al.* 2004. The worldwide leaf economics spectrum. *Nature 2004 428:6985* **428**: 821–827.

Wu J, Chavana-Bryant C, Prohaska N, Serbin SP, Guan K, Albert LP, Yang X, van Leeuwen WJD, Garnello AJ, Martins G, *et al.* 2017. Convergence in relationships between leaf traits, spectra and age across diverse canopy environments and two contrasting tropical forests. *New Phytologist* **214**: 1033–1048.

Wu; J, Prohaska; N, Saleska S. **2019a**. 2012-leaf-reflectance-spectra-of-tropical-trees-in-tapajos-national-forest - Dataset - EcoSIS Spectral Library.

Wu; J, Prohasksa; N, Hough; M, John; A, Garnello; J, Saleska S. **2019b**. 2014-leaf-reflectance-spectra-of-tropical-plants-growing-in-biosphere2 - Dataset - EcoSIS Spectral Library.

Wu J, Rogers A, Albert LP, Ely K, Prohaska N, Wolfe BT, Oliveira RC, Saleska SR, Serbin SP. **2019**. Leaf reflectance spectroscopy captures variation in carboxylation capacity across species, canopy environment and leaf age in lowland moist tropical forests. *New Phytologist* **224**: 663–674.

Wu S, Zeng Y, Hao D, Liu Q, Li J, Chen X, Asrar GR, Yin G, Wen J, Yang B, *et al.* 2021. Quantifying leaf optical properties with spectral invariants theory. *Remote Sensing of Environment* **253**: 112131.

Yan Z, Guo Z, Serbin SP, Song G, Zhao Y, Chen Y, Wu S, Wang J, Wang X, Li J, *et al.* 2021. Spectroscopy outperforms leaf trait relationships for predicting photosynthetic capacity across different forest types. *New Phytologist* **232**: 134–147.

Yang X, Tang J, Mustard JF, Wu J, Zhao K, Serbin S, Lee JE. **2016**. Seasonal variability of multiple leaf traits captured by leaf spectroscopy at two temperate deciduous forests. *Remote Sensing of Environment* **179**: 1–12.

Yang Y, Wang H, Harrison SP, Prentice IC, Wright IJ, Peng C, Lin G. **2019**. Quantifying leaf-trait covariation and its controls across climates and biomes. *New Phytologist* **221**: 155–168.

Yi Q, Wang F, Bao A, Jiapaer G. **2014**. Leaf and canopy water content estimation in cotton using hyperspectral indices and radiative transfer models. *International Journal of Applied Earth Observation and Geoinformation* **33**: 67–75.